GEOSPHERE

GEOSPHERE, v. 20, no. 4

https://doi.org/10.1130/GES02722.1

9 figures; 1 table

CORRESPONDENCE: jplatt@usc.edu

CITATION: Platt, J.P., Grujic, D., Phillips, N.J., Piazolo, S., and Schmidt, D.A., 2024, Geological fingerprints of deep slow earthquakes: A review of field constraints and directions for future research: Geosphere, v. 20, no. 4, p. 981–1004, https://doi.org/10.1130/GES02722.1.

Science Editor: Andrea Hampel
Associate Editor: Francesco Mazzarini

Receive 30 September 2023
Revision received 20 April 2024
Accepted 3 May 2024

Published online 28 May 2024

Geological fingerprints of deep slow earthquakes: A review of field constraints and directions for future research

John P. Platt[1], Djordje Grujic[2], Noah J. Phillips[3], Sandra Piazolo[4], and David A. Schmidt[5]

[1]Department of Earth Sciences, University of Southern California, Los Angeles, California 90098, USA
[2]Department of Earth and Environmental Sciences, Dalhousie University, Halifax, Nova Scotia B3H 4R2, Canada
[3]Department of Geology, Lakehead University, Thunder Bay, Ontario P7B 5E1, Canada
[4]School of Earth and Environment, The University of Leeds, Leeds LS2 9JT, UK
[5]Department of Earth and Space Sciences, University of Washington, Seattle, Washington 98195-1310, USA

ABSTRACT

Slow earthquakes, including low-frequency earthquakes, tremor, and geodetically detected slow-slip events, have been widely detected, most commonly at depths of 40–60 km in active subduction zones around the Pacific Ocean Basin. Rocks exhumed from these depths allow us to search for structures that may initiate slow earthquakes. The evidence for high pore-fluid pressures in subduction zones suggests that they may be associated with hydraulic fractures (e.g., veins) and with metamorphic reactions that release or consume water. Loss of continuity and resulting slip at rates exceeding 10^{-4} m s^{-1} are required to produce the quasi-seismic signature of low-frequency earthquakes, but the subseismic displacement rates require that the slip rate is slowed by a viscous process, such as low permeability, limiting the rate at which fluid can access a propagating fracture. Displacements during individual low-frequency earthquakes are unlikely to exceed 1 mm, but they need to be more than 0.1 mm and act over an area of ~10^5 m^2 to produce a detectable effective seismic moment. This limits candidate structures to those that have lateral dimensions of ~300 m and move in increments of <1 mm. Possible candidates include arrays of sheeted shear veins showing crack-seal structures; dilational arcs in microfold hinges that form crenulation cleavages; brittle-ductile shear zones in which the viscous component of deformation can limit the displacement rate during slow-slip events; slip surfaces coated with materials, such as chlorite or serpentine, that exhibit a transition from velocity-weakening to velocity-strengthening behavior with increasing slip velocity; and block-in-matrix mélanges.

1. INTRODUCTION

Slow earthquakes are displacement events detected geodetically or seismically that occur at slip rates faster than relative plate motions (cm/yr) but slower than classical earthquakes (m/s). They range in scale from low-frequency earthquakes, which may involve displacements of a millimeter or less and durations of a few seconds, up to slow-slip events, detected geodetically, with displacements up to tens of centimeters and durations of hours to weeks (e.g., Miller et al., 2002; Ide et al., 2007a; Frank et al., 2015a). Since their discovery in active subduction zones and transform faults around the Pacific Rim (Obara, 2002; Rogers and Dragert, 2003), there has been considerable debate and speculation as to the precise deformational phenomena that give rise to these signals. The observed slow earthquake characteristics cannot, at present, be reconciled with our current understanding of how rocks deform. Extensively studied ductile deformation mechanisms, such as dislocation creep and diffusion creep, are not compatible with the large range in slip rates of slow earthquakes, yet brittle mechanisms in the strict sense would result in recognizable earthquake signatures faster than those associated with slow earthquakes. To fill this critical gap in our knowledge, we need to search for evidence of the relevant deformation processes in the geological record. Slow earthquakes are abundant in plate-boundary regions, such as subduction zones (Fig. 1), as well as along some transform boundaries (see Section 2), and should leave a distinct imprint in the rocks. Over the last two decades, various processes or combinations of processes, outside the classic ductile versus brittle mechanisms, have been proposed to be responsible for slow earthquakes (see recent reviews by Behr and Bürgmann, 2021; Kirkpatrick et al., 2021).

Numerical models and laboratory friction studies have provided a canonical theory for the origin of these slip phenomena, one where frictional sliding laws dictate the slip behavior (Rubin, 2008; Hawthorne and Rubin, 2013; Barbot, 2019; Im et al., 2020; Lavier et al., 2021). Fluid-pressure variations are clearly implicated, however, as well as fracture propagation in a fluid-rich environment (e.g., Saffer and Tobin, 2011; Frank et al., 2015b; Audet and Schaeffer, 2018; Xing et al., 2019; Chen, 2023). While numerical models and laboratory experiments allow for exploration of potential mechanisms, these methods are hampered by uncertainties in the relevant parameters and boundary conditions and in the possible range of parameters that can be tested. Slow earthquakes are multiscale in length, time, and seismic moment, but laboratory experiments are constrained in scale, and multiscale numerical models remain challenging. One possible avenue to test proposed mechanisms that are responsible for slow earthquake

John Platt https://orcid.org/0000-0002-4459-1864

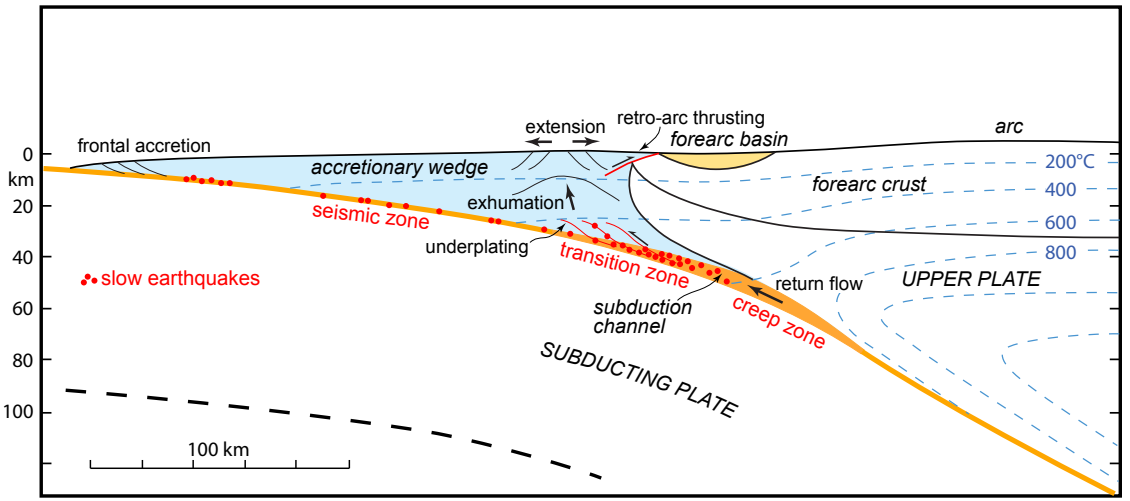

Figure 1. Schematic structural overview of a mature, heavily sedimented subduction zone showing zones of seismic activity, slow earthquakes, and aseismic creep, together with the locations of the main tectonic processes. Isotherms are after Peacock et al. (2011). The deep slow earthquakes discussed in this article occur in the transition zone between the seismic and aseismic creep zones, but slow earthquakes may also occur at shallow levels along the subduction-zone interface and locally within the seismic zone. The subduction-zone interface is shown as an orange line, but at depths below the seismic zone, the subduction channel, which may be several kilometers thick, forms a zone of distributed deformation taking up plate motion.

phenomena is to assess geological structures from areas interpreted to have undergone slow earthquakes in light of their potential geophysical signatures.

So far, no geological structure has been identified that can be directly associated with present-day slow earthquakes. This is because the source regions for these phenomena lie up to 60 km below the surface (Fig. 1). Hence, we need to go to the geological record. Various different geological structures found in deformed rocks from ancient tectonic zones have been implicated, but they are still being heavily debated (e.g., Behr and Bürgmann, 2021; Kirkpatrick et al., 2021). A major challenge is that deformational structures in rocks span a wide range of geometries, as well as temporal and spatial scales, making it difficult to isolate a single common mechanism. The state of preservation and superposition of these structures, and the fact that they represent the end state of a prolonged history of subduction, accretion, and exhumation in subduction zones, complicate the interpretation of the rock record. In April 2022, a Penrose Conference was held on Catalina Island (California) to discuss the possible geological signatures of slow earthquakes, and this review article was conceived as a way of summarizing some of the outcomes of the workshop.

The aim of this article is to describe and illustrate geological structures that have been proposed as signatures of slow earthquakes as a resource for seismologists, geodesists, and geologists who investigate these phenomena. We hope by this means to foster rigorous tests on whether these structures are viable sources of the geodetic and geophysical signals defining slow slip. We start by outlining the tectonic setting of slow earthquakes; we then summarize their main geophysical characteristics and then discuss and illustrate the main classes of structures that have been proposed as potential signatures of slow earthquakes. We finish by discussing the geophysical and geodetic constraints on the temporal and physical scales of slow earthquake sources, and possible deformational phenomena that have not yet been considered as potential sources. To push our understanding of slow earthquakes further, multidisciplinary research efforts are needed with continuous testing and refinement of experimental and theoretical models against observations from the geological record and vice versa.

2. TECTONIC SETTING OF SLOW EARTHQUAKES

Slow earthquakes encompass a variety of deformational phenomena with a wide range of temporal and spatial scales, and they do not all occur in the same tectonic settings. They were first recorded geodetically from active convergent margins, most notably the Cascadia and Nankai Trough subduction zones (Hirose et al., 1999; Dragert et al., 2001; Miller et al., 2002), and they were commonly found to be accompanied by nonvolcanic tremor (Obara, 2002). Embedded within the tremor, impulsive seismic emissions were identified with energy spanning varied frequencies. This family of seismic sources was subdivided based on the frequency range of the dominant seismic waves, with very low-frequency earthquakes in the 0.01–0.1 Hz frequency band and low-frequency earthquakes in the 1–10 Hz range (Beroza and Ide, 2011). Both very low-frequency earthquakes and low-frequency earthquakes are depleted in the higher-frequency energy commonly observed from regular earthquakes. It has subsequently been proposed that the tremor is composed of a series of concatenated low-frequency earthquakes and very low-frequency earthquakes (Ide et al., 2007a; Shelly et al., 2007; Frank et al., 2016, 2018). Isolated low-frequency earthquakes and very low-frequency earthquakes, not associated with slow-slip events, can also occur in these settings.

Slow earthquakes, and the accompanying family of seismic events, are found in subduction zones both updip and downdip of the seismogenic zone. On the Cascadia margin, slow-slip and tremor events are very clearly located in a zone along or close to the subduction zone interface and downdip of the seismogenic zone, at depths between 40 km and 60 km (Hirose et al., 1999; Dragert et al., 2001; Obara, 2002), and separated from the seismically active region by a distinct quiet zone (Bartlow, 2020). On the Guerrero margin in Central America, by contrast, tremor events and slow slip occur within the seismically active zone, possibly filling in the gaps between seismic asperities, although the most abundant tremor events lie downdip from the seismic zone (Frank et al., 2015b). On both the Hikurangi and Costa Rica margins, slow earthquakes and tremor events have been identified at depths of <15 km (Wallace, 2020; Baba et al., 2021), where conditions are distinct from those accompanying deeper slow earthquakes found on other subduction systems (Saffer and Wallace, 2015). The expansion of seafloor geophysical arrays in the Nankai and Japan troughs has revealed a complex distribution of shallow tremor and other slow earthquake phenomena (Tamaribuchi et al., 2022; Nishikawa et al., 2023). Slow earthquakes in the shallow parts of accretionary wedges may reflect low effective stress, the frictional properties of clay minerals, and a heterogeneous fault interface, producing a fault zone with conditional frictional stability and low rigidity (Saffer and Wallace, 2015).

Subduction-related slow earthquake events almost all occur in Pacific margin settings, such as the Aleutian arc, Cascadia, Central America, Japan Trench, Nankai Trough, and the Hikurangi margin. In most of these areas, siliciclastic sediment is being deposited in the related deep-sea trenches (Scholl, 2019), and it is being accreted to and subducted beneath the accretionary wedge, which suggests that the presence of abundant water-saturated sediment may favor slow-slip behavior. Slow earthquake events have not been recorded from continental collision zones or subduction zones associated with Alpine-Himalayan convergent margins. This may partly reflect the scarcity of seismic or geodetic networks capable of detecting these signals, but it may indicate that crystalline basement rocks and passive-margin sedimentary sequences do not produce these signals.

Tremor events have been identified along some transform margins, most notably on the San Andreas fault, where these signals occur at depths of 25–30 km, below the seismically active zone, in central California (Shelly, 2009). Geodetically detected slow-slip events have also been identified along that section of the San Andreas fault (Rousset et al., 2019), and both slow-slip and tremor events have been identified along the Alpine fault in New Zealand at depths between 17 km and 42 km (Baratin et al., 2018). Initial estimates of low-frequency earthquake focal mechanisms suggested quasi-continuous shear faulting with one nodal plane nearly parallel to the Alpine fault and primarily dextral strike-slip motion with minor reverse slip. The low-frequency earthquakes fill a seismicity gap between shallow (0–12 km) and deep (50–100 km) seismic events, occurring in a zone characterized by high seismic reflectivity, low seismic-wave speeds, and elevated fluid pressure that may reflect metamorphic reactions at depth (Saffer and Tobin, 2011; Chapman et al., 2022).

In summary, slow earthquake phenomena are widely observed on active plate boundaries, particularly oceanic subduction zones where water-rich sediments are subducted, and they are likely to represent a prevalent geological process. This suggests that slow earthquakes should be widely represented in the rock record and associated with a common set of deformational mechanisms. Most of the discussion in this article relates to geologically identifiable structures in rocks that have been exhumed from depths of 20–50 km in young or active subduction-zone settings (Fig. 1), as these can be most clearly related to the environment in which the whole range of slow earthquake phenomena has been most abundantly documented.

3. SIGNATURES OF SLOW EARTHQUAKES IN THE GEOLOGICAL RECORD

In our discussion, we have to take into account the range of spatial and temporal scales implied by the geophysical and geodetic signals of slow earthquakes. Low-frequency earthquakes may well be associated with structures that can be observed in outcrop, with displacements of 1 mm or less and dimensions of a few hundred meters (e.g., Chestler and Creager, 2017). Much of our discussion in this paper therefore relates to the possible geological signatures of low-frequency earthquakes.

Geodetically observable slow-slip events, by contrast, may be generated by structures tens of kilometers in extent in the displacement direction and hundreds of kilometers in extent normal to the displacement (e.g., Houston et al., 2011). Structures on this scale can be difficult to identify and delineate in the field. Given the difference in scale, it is possible that slow-slip events and low-frequency earthquakes may originate from different regions within the same zone of deformation. Slow-slip events could originate from quite a large volume, whereas low-frequency earthquakes are likely more discrete in time and space.

A particularly difficult issue is the rate of displacement, which is the defining feature of slow earthquakes. Displacement rates can be determined directly by geodesy and inferred from the effective moment of low-frequency earthquakes, but the rate and time scale on which geological structures are formed are notoriously difficult to determine from field-based observations. Geochronological techniques have insufficient resolution to solve the problem, though some estimates can be made about the time scales on which fractures heal from the solubility and diffusivity of the materials deposited within them.

Another problematic issue facing the field geologist is the role of the subduction-zone megathrust. From a geophysical perspective, this is a continuous discrete slip surface that extends to depths of around 80 km, at which the subducting slab becomes viscously coupled to the mantle wedge. Structural investigations in accretionary complexes that have been exhumed from the seismogenic zone have identified zones of cataclasis a few hundred meters thick with pseudotachylite veins indicating seismic slip (e.g., Rowe et al., 2005, 2013). However, in terranes exhumed from 30 km depth or more, deformation

is more broadly distributed, and it has occurred largely by viscous processes, such as dissolution-precipitation creep and dislocation creep (e.g., Behr and Platt, 2013; Ujiie et al., 2018; Condit and French, 2022; Schmidt and Platt, 2022; Tulley et al., 2022). The field geologist sees the end state of the whole geological history, however, so an apparently distributed zone of deformation may in fact comprise a whole array of discrete slip or high-strain zones (e.g., Gardner et al., 2017). Discrete slip surfaces are hard to find, and if they do not show evidence of seismic slip, such as pseudotachylite, slip rates are difficult to determine. In general, the geological evidence suggests that discrete frictional slip surfaces do not extend to depths much beyond the frictional-viscous transition; below that, most of the displacement takes place by distributed deformation over a zone that may be hundreds of meters to several kilometers thick.

An additional complication is that the preservation and eventual exhumation of rocks from depths of 30 km or more require underplating, which means that the megathrust has occupied progressively lower positions relative to the accreted rock (Fig. 1). These successive positions of the megathrust may correspond to the so-called terrane boundaries in exhumed accretionary complexes, such as the Franciscan Complex in California (Schmidt and Platt, 2018; see thrust faults highlighted in red in Fig. 2). They may show discontinuities in metamorphic conditions and structural style, and they are commonly occupied by zones of disrupted material derived from the surrounding units (mélange) but rarely show evidence of seismic activity.

When estimating the type of geophysical signal that a given structure or set of structures might have produced, we need to know how they were oriented relative to the subduction zone as a whole. The structures we see in the field reflect the superposition of deformation during subduction, underplating, and exhumation, which can tilt and rotate the rocks around a wide range of axes (Platt, 2000). Exhumation processes, in particular, may introduce large- and small-scale structures that complicate the geometry. Our inferences about the tectonic significance of a given set of structures are therefore subject to substantial uncertainty.

The geological structures we consider fall into three main groups, described in Sections 4, 5, and 6. Group 1 comprises structures formed by dilational cracking, including various types of veins. It forms a large and potentially very important group, as these structures form under conditions of high fluid pressure, which several lines of evidence indicate is likely to favor slow earthquakes. High fluid pressures require specific patterns of porosity and permeability within structures and raise questions about the sources of the fluids. Group 2 relates to structures formed in viscous or brittle-viscous shear zones. We treat these together, as they commonly evolve from one to the other, alternate, or operate together under the conditions we are considering, and the change from brittle to viscous behavior, or vice versa, depends strongly on rock type, fluid pressure, and differential stress. Group 3 consists of structures formed by localized or distributed brittle faulting, which correspond most closely to the geophysical concept of slow earthquakes as a phenomenon explicable in terms of rate-and-state friction. We group block-in-matrix mélanges under this heading, although they may also show characteristics of group 2. While we discuss the structures in each group individually, it is likely that structures from different groups may coexist within a volume of rock. In the following sections, we put the three groups of structures in the context of slow earthquakes, and we discuss the mechanistic background. The overall tectonic setting of these structures is shown in Figure 1, the local structural context for some of them are shown in Figure 2, and the structures themselves are illustrated in Figures 3–8.

4. STRUCTURES FORMED BY DILATIONAL CRACKING

There is considerable geophysical evidence suggesting that the oceanic crust and overlying sediment in active subduction zones experience high pore-fluid pressures, possibly approaching lithostatic, and high fluid pressures may also exist at depth along major strike-slip faults. The evidence includes high Vp/Vs ratios and high attenuation of seismic P-waves (Audet et al., 2009; Beroza and Ide, 2011; Kitajima and Saffer, 2012; Wech et al., 2012; Audet and Bürgmann, 2014; Audet and Schaeffer, 2018; Savard et al., 2018; Calvert et al., 2020), triggering of slow-slip events by tidal stresses and teleseismic events (Thomas et al., 2009; Peng and Gomberg, 2010; Johnson et al., 2013; Houston, 2015), and low stress drops associated with low-frequency earthquakes and tremor events (Gao et al., 2012; Bostock et al., 2015; Chestler and Creager, 2017). Low stress drops and tidal and teleseismic triggering are most easily explained by high fluid pressures, which reduce the shear stresses required for frictional slip (Sibson, 2017). Rocks exhumed in accretionary complexes also show abundant evidence for high pore-fluid pressures in the form of veins and other dilational fractures (Figs. 3 and 4). These may be filled with minerals such as quartz, calcite (Meneghini et al., 2007; Fagereng et al., 2011; Fagereng and Harris, 2014; Fisher and Brantley, 2014; Bons et al., 2012; Cerchiari et al., 2020; Ujiie et al., 2018), garnet (e.g., Taetz et al., 2018; Spandler and Hermann, 2006), or serpentine (Andreani et al., 2004; Tarling et al., 2019), in which case they are recognizable in the geological record. As a result, these structures are commonly cited as possible signatures of slow-slip events.

The source of the fluid required to produce these veins, and whether it is local or derived from depth within the subduction zone, is a topic of considerable importance. At shallow levels in the subduction zone, compaction of sediment, particularly of young, high-porosity trench sediments, will produce large volumes of water. Temperature-dependent dehydration reactions of clay minerals and chlorite (to micas, glaucophane, and, at higher temperatures, garnet), lawsonite (to epidote), and glaucophane (to omphacite) occur progressively at greater depths and hence temperatures (for an extensive review, see Behr and Bürgmann, 2021). Links between specific dehydration reactions and slow earthquakes have not been established, but the generation of high fluid pressures in subduction zones must clearly be responsible for modifying the mechanical properties of the rocks involved.

Precipitation of large amounts of quartz presents problems in that the solubility of silica in water in subduction-zone environments is on the order of

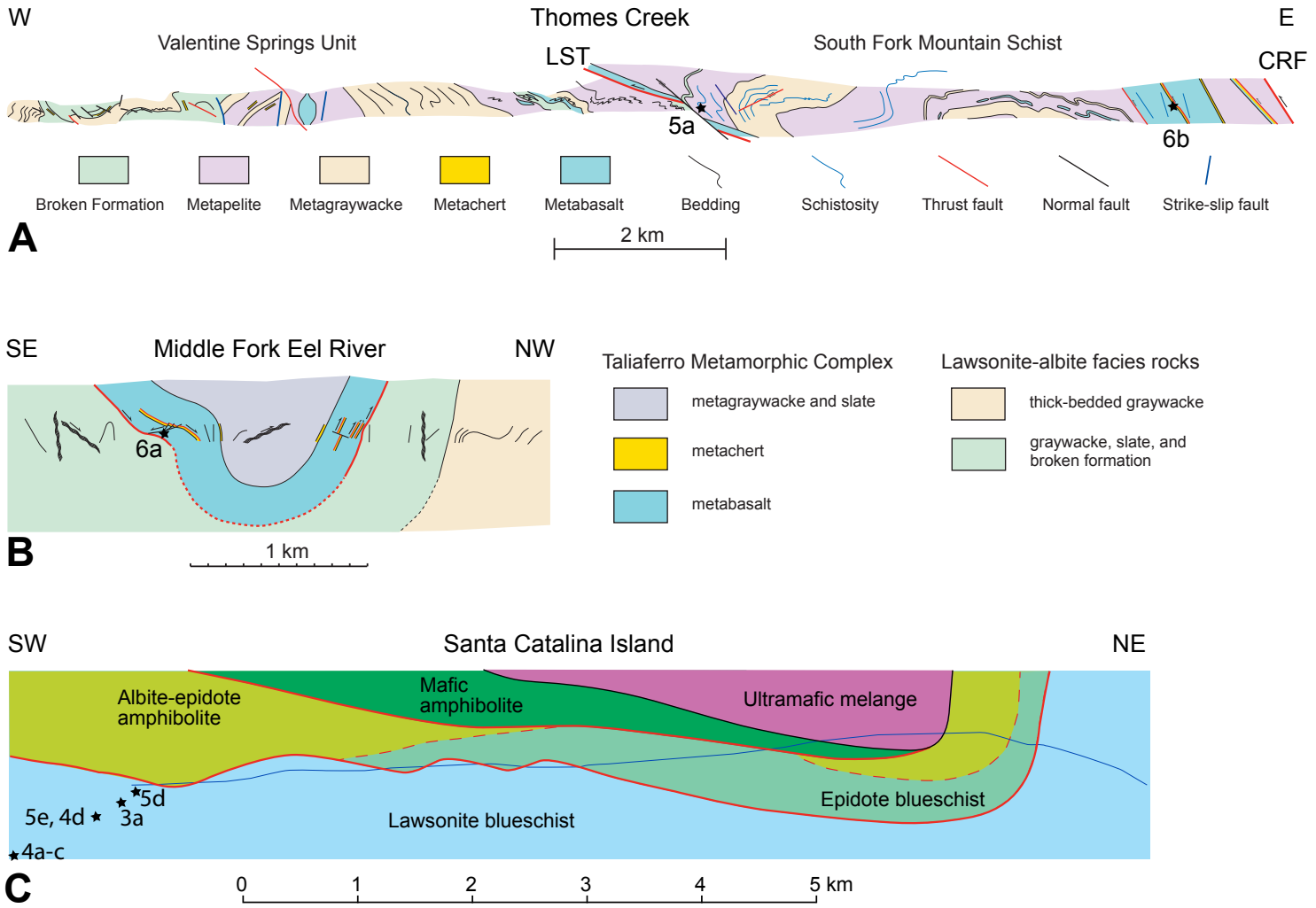

Figure 2. Cross sections showing the location and setting of some of the structures illustrated in this paper (stars with figure numbers). (A) Section along Thomes Creek and (B) section in the Middle Fork of the Eel River, both in the Eastern belt of the Franciscan Complex in the northern California Coast Ranges, after Schmidt and Platt (2018). Section B lies west of and structurally below section A. In section A, CRF is the Coast Range fault, which marks the oldest and highest position of the subduction-zone megathrust, and LST is the Log Spring thrust, which marks the next position down of the megathrust. The rocks between the two faults comprise the blueschist-facies South Fork Mountain Schist, which was accreted ca. 121 Ma (Dumitru et al., 2010); the rocks below the LST are in the lawsonite-albite facies and were accreted ca. 117 Ma (Lanphere et al., 1978). In section B, the blueschist-facies Taliaferro metamorphic complex overlies lawsonite-albite–facies rocks along a thrust that may be of the same age or slightly younger than the LST. (C) Section across Santa Catalina Island in the southern California borderland. A sequence of tectonic units that decrease downward in age and metamorphic grade was progressively underplated in the period 115–100 Ma (Platt et al., 2020; Platt and Schmidt, 2024).

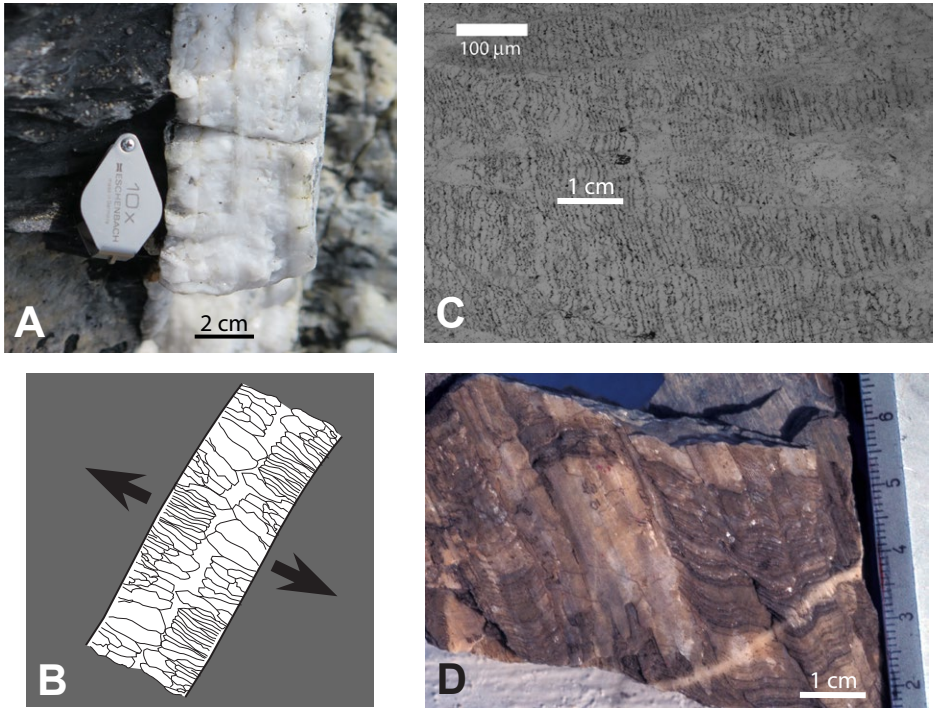

Figure 3. Mode 1 (dilational) veins. (A) Quartz vein with syntaxial growth microstructure, Cottonwood Beach, Catalina (33.3761°N, 118.4765°W). Note the distinct median zone, the columnar structure on either side, and the structureless quartz along the boundaries. Blueschist facies, 330 °C, 1.1 GPa (Platt et al., 2020). Dilational veins like these require fluid pressures close to lithostatic, which has been widely suggested to be associated with slow earthquakes. (B) Quartz vein, showing syntaxial growth of quartz crystals from the margin toward the center into a fluid-filled cavity. The quartz crystals have faceted terminations; the void space along the center line may be filled with quartz or other minerals. This requires the maintenance of high fluid pressures for enough time to allow vein filling. Sketch is based loosely on figure 1a of Bons et al. (2012). (C) Crack-seal microstructure in quartz vein. Regularly spaced inclusion bands composed of phyllosilicates similar to those in the wall rock indicate repeated fracture with 8 µm spacing (from Fisher and Brantley, 2014). (D) Crack-seal increments with 0.2–0.5 mm spacing in calcite vein, Makran accretionary prism, SW Pakistan (25.4261°N, 63.7277°E). The vein is a shear vein, but the crack-seal structure shows that it formed by dilational fracturing. These individual increments of dilational fracturing have displacements compatible with low-frequency earthquakes. Burial depth ~5 km. Photos in A and D are by John Platt.

100–1000 ppm (Williams and Fagereng, 2022). If transport of silica is advective, very large volumes of fluid are required, which would have to come from an external source. Sequences of thick veins, such as those shown in Figure 4A, almost certainly require large fluxes of water. The source for these is likely to be dehydration reactions deeper in the subduction zone (e.g., Fagereng and Diener, 2011; Condit et al., 2020), and this is supported by geochemical data (Cerchiari et al., 2020). If silica is transported by diffusion, the rate of sealing of the veins is limited by the diffusivity of silica through the host rock. In many examples, vein formation can be shown to be coeval with pressure-solution (dissolution-precipitation) creep in the surrounding rock, contributing to cleavage formation (Meneghini et al., 2007; Fagereng and den Hartog, 2016; Ujiie et al., 2018; Schmidt and Platt, 2022), but the slow rate at which silica can be deposited means that filling of veins a centimeter or more thick is likely to take place on time scales that are long compared to the seismic cycle or to the frequency of slow-slip events (Williams and Fagereng, 2022). This suggests that only veinlets or individual crack-seal increments a few tens of microns thick can plausibly be related to individual seismic or low-frequency earthquake events.

Various different vein geometries have been observed, with different modes of formation and relationships to regional stress. These are discussed in the following subsections.

4.1 Mode 1 Veins with Syntaxial and Antitaxial Opening

Mode 1 (or tensile) veins are thought to form by hydraulic fracturing when the pore-fluid pressure, P_f, exceeds the least compressive stress (σ_3) by the tensile strength of the rock, and they open in the direction of σ_3. The direction of opening is indicated by the columnar geometry of the grains (Figs. 3A and 3B). These may nucleate on the vein walls and then grow toward the vein center as it progressively opens by repeated fracture in the center of the vein (syntaxial growth; Fisher et al., 1995). Alternatively, fracture may occur on one or both vein margins, so that the crystals grow out toward the margins (antitaxial growth; Bons et al., 2012). Opening is incremental, and the opening increments may be visible in the form of crack-seal textures, where the increments, commonly 5–100 µm, are rendered visible by trains of inclusions within the relatively coarse grains that make up the veins (Figs. 3C and 3D; Ramsay, 1980; Fagereng et al., 2011; Fisher and Brantley, 2014). These inclusions may be fragments of wall-rock grain spalled off during the cracking event or slivers of minerals, such as mica or chlorite, that grew during the sealing event (Cox and Etheridge, 1983). Intragranular to transgranular microfractures may also be outlined by planar arrays of fluid inclusions, which may represent mode 1 fractures that have subsequently healed. The time required for healing can

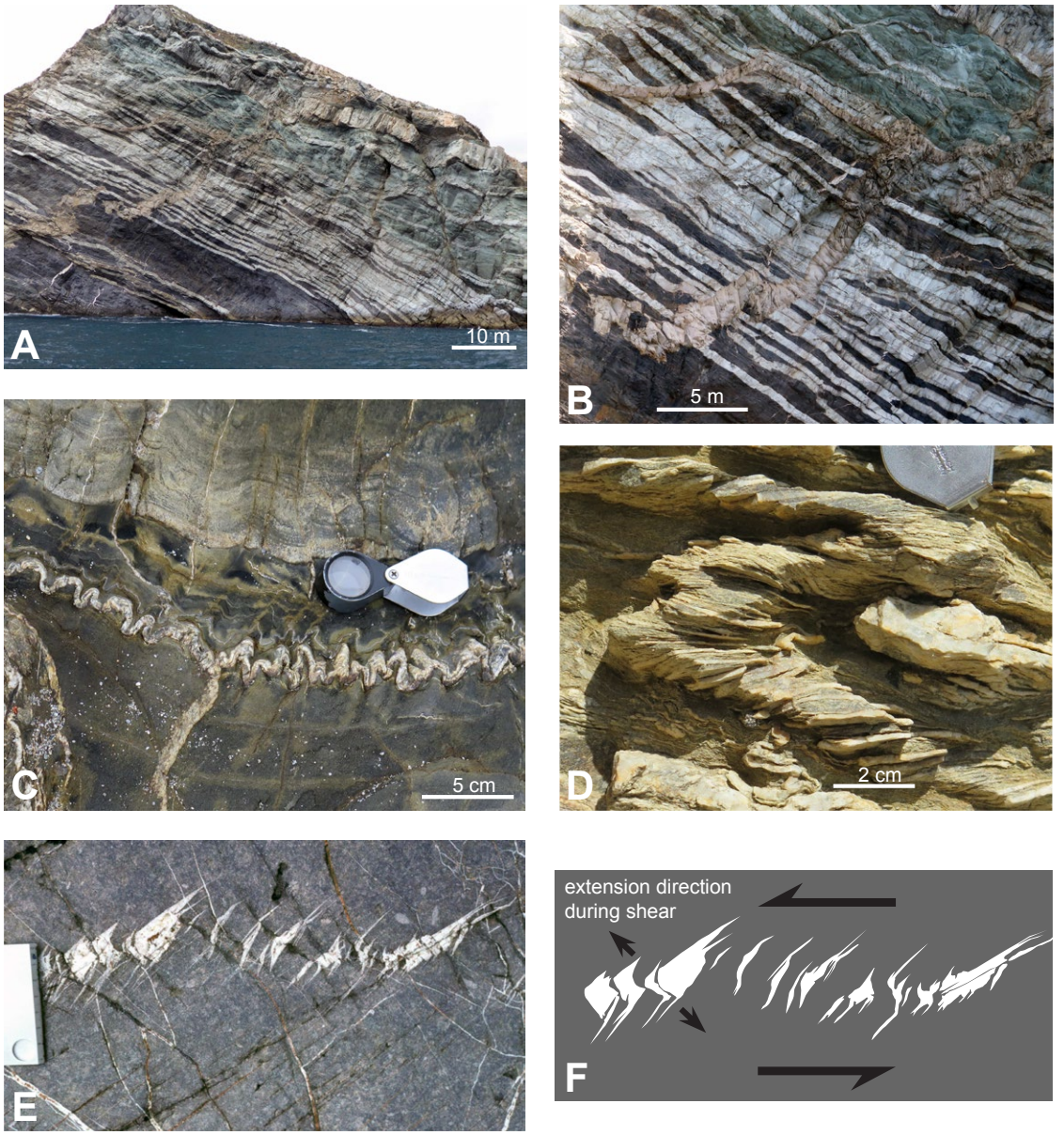

Figure 4. (A) Mode 1 sheeted quartz vein complex, Ribbon Rock, Catalina (33.4388°N, 118.5727°W). The cliff is 50 m high. Lawsonite-albite facies. (B) Detail. Many of the veins are composite and cut each other at low angles. The scale of these veins requires the transport of very large quantities of fluid. The veins are Late Cretaceous, and they are crosscut by a beige Miocene silicic dike. (C) Folded mode 1 quartz vein, Starlight beach, Catalina (33.4750°N, 118.5896°W). The vein was emplaced parallel to bedding in graywacke sandstone and shale, and it lies in the hinge of a later upright meter-scale fold. This demonstrates the alternation of dilational fracture formation and ductile deformation. Lawsonite-albite facies. (D) Millimeter-scale mode 1 quartz veins within folded metagraywacke track the axial-plane cleavage of the fold, Ben Weston beach, Catalina (33.3669°N, 118.4820°W). Blueschist facies, 330 °C, 1.1 GPa (Platt et al., 2020). (E) En échelon vein array in a brittle-ductile shear zone, Carboniferous pebbly sandstone, Millook Haven, SW England (50.7722°N, 4.5754°W). The veins formed in a zone of ductile shear (top to left) normal to the direction of extension, and they were deformed into a sigmoidal shape by continuing shear. Burial depth 6–8 km. (F) Sketch based on the structures in E, showing their relationship to the shear zone. The oldest parts of the veins have been rotated by shear, but the veins have continued to propagate normal to the instantaneous extension direction in the shear zone. Fracture propagation is rate-limited by the rate of shear in the viscous matrix, fracture dilation by the permeability of the matrix, and fracture filling by the diffusivity of silica in solution. The association in time of brittle and viscous deformation provides a mechanism for producing rate-limited slow earthquakes. All photos are by John Platt.

range from a few hours (Smith and Evans, 1984; Brantley et al., 1990; Brantley, 1992) to a few days (Fisher and Brantley, 2014) and initiates from the crack tip. This model assumes that the high surface curvature at the fracture tip causes changes in chemical potential, leading to mass transport.

An alternative mode of vein growth occurs if the vein and the interface are stronger than the host rock. New fractures then tend to form in the host rock adjacent to an existing vein. Repeated fracturing and sealing can produce sets of parallel veins, with single-event hair-like veins generally <100 µm thick reflecting the aperture of a single fracture event. In this case, the crystals in the vein will grow from one side to the other (antitaxial growth). This repeated delocalized fracturing of a veined rock is known as the crack-jump mechanism (Caputo and Hancock, 1999).

Multiple mode 1 veins may form sheeted vein complexes up to tens of meters thick (Figs. 4A and 4B), which can represent significant extensional strain normal to the foliation. It is generally accepted that propagation of mode 1 veins requires fluid pressures in excess of lithostatic, but vein opening is likely to cause a drop in fluid pressure, which limits the amount of opening (Segall et al., 2010). If opening ceases, the vein is healed, and there is a continuous resupply of fluid, then the process can repeat itself at intervals modulated by the permeability of the surrounding rock (Fisher et al., 1995; Meneghini and Moore, 2007; Ujiie et al., 2018; Condit and French, 2022; Williams and Fagereng, 2022), which may explain the repeating character of low-frequency earthquakes (see Section 7.2).

Mode 1 veins may cut at high angles across layering or foliation in the host rock, or they may form parallel to the layering, depending on the orientation of the layering relative to the principal stresses. They are likely to open in the direction of the minimum principal stress, and hence the maximum principal stress lies in the plane of the veins. Continued bulk shortening of the rock within the plane of the veins may therefore produce buckle folds, as the veins are commonly stronger than the host rock (Fig. 4C). Their orientation may also be controlled by a preexisting foliation, including axial-plane cleavage in folded rocks (Fig. 4D).

The displacements, lateral extent, and abundance of mode 1 veins make them a plausible candidate source for low-frequency earthquakes, but the seismic evidence indicates that low-frequency earthquakes represent double-couple shear events with a low-angle thrust sense (Ide et al., 2007b), which may be incompatible with them being mode 1 fractures. Some dilational veins form en échelon sets within what is otherwise a zone of distributed ductile shear (Beach, 1975; Condit and French, 2022) and, hence, may be compatible with the seismic evidence. These veins are commonly folded into sigmoidal shapes by coeval propagation of the vein and rotation of the older part of the vein during continuing shear (Figs. 4E and 4F). En échelon vein sets represent an example of mixed frictional and viscous deformation where the rate of opening of the veins is controlled by the viscous strain rate in the surrounding rock. The mixed-mode deformation involved, and their occurrence in shear zones, is consistent with these structures being a low-frequency earthquake source, but their limited length and restricted occurrence argue against them making more than a very minor contribution to the overall motion along a plate boundary.

4.2 Fiber-Lineated Shear Veins

These are essentially mode 2 shear fractures, but with a component of opening normal to the fracture surface. The opening may be a result of a step in the fracture surface, in which case, the vein may not be present along the entire fracture surface (Fig. 5A). Crystal growth in the vein takes place parallel to the direction of motion, so that the fibers are subparallel to the plane of the fracture. The elongate crystal fibers commonly show crack-seal increments of growth (Fig. 5B; Platt et al., 1988; Fagereng et al., 2011; Giuntoli and Viola, 2022), and their orientation may track the slip history on the fault (Fig. 5C). Shear veins, like mode 1 veins, can form sheeted vein complexes (Figs. 5D and 5E). These may accommodate significant shear displacement, and they commonly occur along major thrust surfaces (Fig. 2; see also Schmidt and Platt, 2018). Continued shear in these vein complexes may result in asymmetric buckle folding of the veins (Fig. 4D), and some sheeted vein complexes become intensely folded as a result of a transition into distributed ductile shear (Fig. 5E).

Sibson (2017) has suggested that the combination of slip on the shear fractures and dilational opening at the steps constitutes a viscoplastic (dashpot-slider) rheological combination. If the viscous and plastic behavior act in parallel, then these are Bingham materials, which display linear viscous behavior only above a yield-stress value, such as that characterizing plastic materials (Sibson, 2017, fig. 11), and this could explain slow earthquakes. Fagereng et al. (2011) pointed out that the presence of crack-seal increments of growth indicates that a single shear surface can produce a slip event that repeats itself hundreds to thousands of times, which is a characteristic of low-frequency earthquakes. The displacements, lateral extent, and abundance of mode 2 shear veins make them a plausible candidate source for low-frequency earthquakes, and the sense of displacement is compatible with the seismic evidence for a double-couple mechanism.

4.3 Dilational Arcs in Microfold Hinges

In strongly foliated rocks (slates and schists), dilational arcs can form in the short limbs or hinges of kink-bands or microfolds (crenulations), as a result of the strain incompatibilities in the material as the plane of anisotropy is rotated by the folding (Schmidt and Platt, 2022). Displacements are commonly of the order of 1 mm, depending on the scale of the microfolding, but the crenulation band as a whole may represent a shear displacement of as much as 1 cm (Fig. 5F; for the structural context, see Fig. 2). Multiple subparallel kink or crenulation bands commonly form, defining axial planar crenulation cleavages to larger-scale folds. The rate of displacement is limited in the same way as it is for other dilational fractures by the need to diffuse fluid into

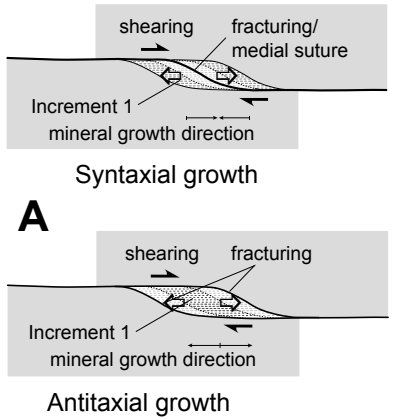

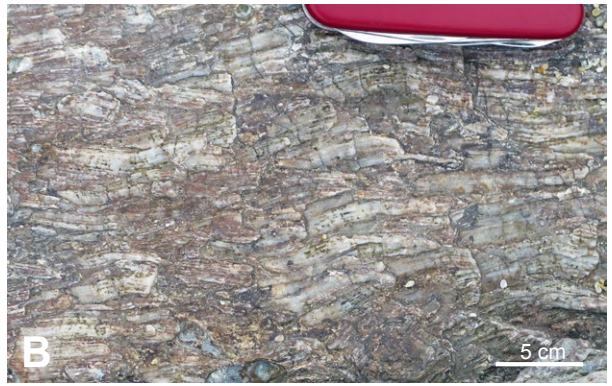

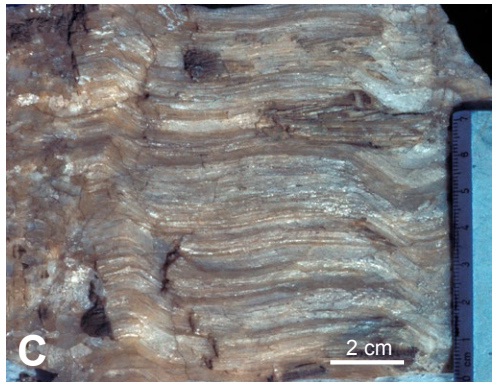

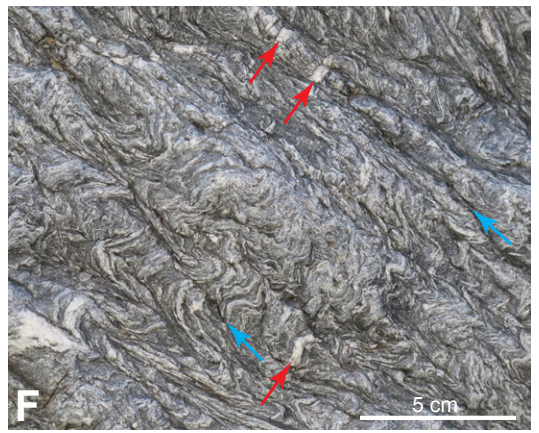

Figure 5. Mode 2 shear veins. (A) Diagrams showing how fiber-lineated shear veins form by dilational fracturing on a releasing step, with syntaxial growth (upper diagram) and antitaxial growth (lower diagram). (B) Fiber-lineated quartz shear vein, Chrystalls beach, Otago, New Zealand (46.1897°S, 170.1155°E). The image is of the surface of the vein, which occupies the whole photograph. The veins lie along discrete shears cutting mélange, visible in Figure 6E. <300 °C, 0.4–0.6 GPa (Fagereng et al., 2011). (C) Fiber-lineated calcite shear vein, Makran accretionary prism, SW Pakistan. The image is of the surface of the vein. The growth fibers tracked the displacement direction, which oscillated between the plate motion direction and the topographic gradient (Platt et al., 1988). The progressive growth of these fibers requires small increments of slip, which could be associated with slow earthquakes. Burial depth ~5 km. (D) Sheeted shear vein complex with asymmetric folds, Shark Bay, Catalina (33.3810°N, 118.4761°W). The vein complex is ~2 m thick and can be traced for ~20 m. The folds resulted from continuing ductile shear after vein formation. Blueschist facies, 330 °C, 1.1 GPa (Platt et al., 2020). (E) Intensely folded sheeted shear vein complex, Ben Weston beach, Catalina (33.3664°N, 118.4699°W). The vein complex is ~2 m thick and can be traced for ~40 m. Vein formation was followed by intense ductile shear producing the folding. The association in time of brittle and viscous deformation provides a mechanism for producing rate-limited slow earthquakes. Blueschist facies, 330 °C, 1.1 GPa (Platt et al., 2020). (F) Dilational arcs in microfolds, Franciscan Complex, Thomes Creek, northern California Coast Ranges (39.8673°N, 122.7480°W). Quartz has filled millimeter-scale dilational zones in the microfold hinges (red arrows). Many of the thinner quartz bands formed in the same way but were folded during continuing deformation. A broadly spaced pressure-solution cleavage developed along the limbs of the microfolds (blue arrows). Blueschist facies, 323 °C, 1.2 GPa (Schmidt and Platt, 2022). All photos are by John Platt.

the dilational cracks. The overall displacement during formation consists of shear parallel to the kink-band (Schmidt and Platt, 2022). The limitation on displacement and displacement rate, and the fact that they act as small-scale shear bands, makes them a plausible candidate source for low-frequency earthquakes (Platt et al., 2018).

5. STRUCTURES IN VISCOUS OR BRITTLE-VISCOUS SHEAR ZONES

Shear zones can exist on a wide variety of scales, and so they may provide us with a window into the possible deformational structures associated with large-scale, geodetically observable slow-slip events. They form a continuum between purely brittle and purely viscous end members. Purely brittle shear zones consist of sets of anastomosing frictional shear surfaces on scales ranging up to the dimensions of the shear zone as a whole. Mechanically, such shear zones will show pressure-dependent behavior, obeying a Coulomb-type friction law, and they may show properties governed by rate-and-state friction (see Section 6). Purely viscous shear zones may form by distributed viscous deformation mechanisms, such as dislocation creep or dissolution-precipitation creep, which are not strongly pressure sensitive, and in general will show a positive relationship between stress and strain rate analogous to velocity-strengthening behavior in a brittle material. In both cases, initiation of the shear zone requires some sort of strain-induced weakening. In a brittle material, this may take the form of loss of cohesion, or one of several forms of velocity-weakening behavior. In a viscous shear zone, weakening may involve precursor brittle fracture (e.g., Fusseis et al., 2006; Mancktelow and Pennacchioni, 2005), or it may result from grain-size reduction (e.g., Svahnberg and Piazolo, 2010; Platt and Behr, 2011), formation of weaker phases by metamorphic reaction (e.g., Brodie and Rutter, 1987; Wintsch et al., 1995), or formation of a shape or crystallographic preferred orientation (e.g., Muto et al., 2011). In both brittle and viscous shear zones, shear heating may play a role (e.g., Kaus and Podladchikov, 2006), and it may cause an increase in the fluid pressure, which may weaken and change the mechanical properties of the shear zone.

In the context of slow earthquakes, the most important aspect of these shear zones is their potential ability to switch from ductile (viscous) to brittle behavior, which could be induced by a change in pore-fluid pressure. Verberne et al. (2017) demonstrated that the transition from flow to friction in experimentally simulated faults is marked by a shift from dislocation and diffusion creep to dilatant deformation, involving grain boundary sliding. Although the transition from purely ductile to frictional-viscous flow occurs gradually, the shift to entirely frictional slip is sudden. This latter phase is distinguished by a linear relationship between shear stress and effective normal stress, along with velocity-weakening behavior. Crucially, the switch from stable shear zone flow to frictional fault slip is predominantly governed by cavitation at the grain scale (intergranular dilatation).

Figure 6A shows an example of this type of deformation mechanism switch. A mode 1 quartz vein with a columnar texture formed by dilational fracture and precipitation of quartz has subsequently been deformed by dislocation creep, as evidenced by lattice distortion, subgrains, and localized dynamic recrystallization. The sample comes from a sheeted vein complex along a thrust surface in the Franciscan Complex of the northern Coast Ranges of California (for the structural context, see Fig. 2). Elsewhere in the same vein complex, there are veins that are so strongly deformed and recrystallized that they are barely recognizable, and these are cut by veins that are largely undeformed. These relationships result from an alternation between a brittle mechanism (dilational fracture) and a viscous mechanism (dislocation creep). This process involves cyclicity in the state of stress; dilational fracture requires high fluid pressure, and hence low effective normal stress and low shear stress (possibly <1 MPa), whereas dislocation creep at temperatures in the 300–500 °C range typically requires differential stresses in the range 30–200 MPa (Behr and Platt, 2014).

Another example on a larger scale is shown in Figure 6B. This is an accretionary thrust zone with a displacement of several kilometers in the South Fork Mountain Schist (Franciscan Complex, northern Coast Ranges of California). The fault zone is 2 m thick, and it shows high ductile strain as well as dilational fracturing to produce quartz veins. Older veins have been rotated and stretched by ductile strain, and younger ones crosscut them at a high angle. Discrete throughgoing faults have accommodated a significant part of the deformation.

If brittle deformation and viscous deformation in these shear zones operate simultaneously and spatially in series, as in a Bingham viscoplastic material, then this provides a potential mechanism for limiting displacement and displacement rate during individual slip events. This raises the question of whether the strain rates produced by the viscous component of deformation are compatible with the displacement rates observed geodetically during slow earthquakes. If the stress and temperature are known, strain rates can in principle be calculated from experimentally determined flow laws for different viscous deformation mechanisms, such as dislocation creep or pressure-solution creep (e.g., Behr and Platt, 2013; Schmidt and Platt, 2022). These flow laws are known with varying degrees of confidence. To calculate displacement rates from strain rates, we need to know the thickness of the active shear zone. This can be measured in the field, but it is not always clear how much of the observed shear zone was active at any given time; this is complicated further if viscous and brittle mechanisms were active at the same time or alternating in time.

6. LOCALIZED OR DISTRIBUTED BRITTLE FAULTING

The combination of near-lithostatic pore-fluid pressures observed through geophysical methods (e.g., Audet et al., 2009; Audet and Kim, 2016), the sensitivity of tremor and slow-slip events to small-scale stress perturbations (e.g., tidal triggering; Miyazawa and Brodsky, 2008; Houston, 2015), and the double-couple focal mechanisms for low-frequency earthquakes (Ide et al., 2007b)

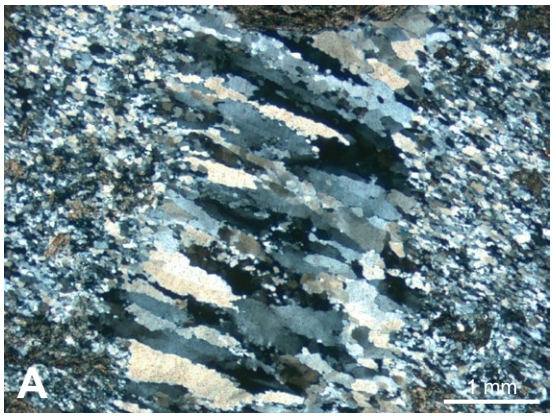

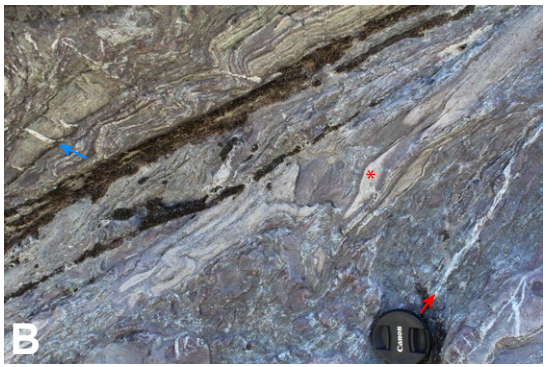

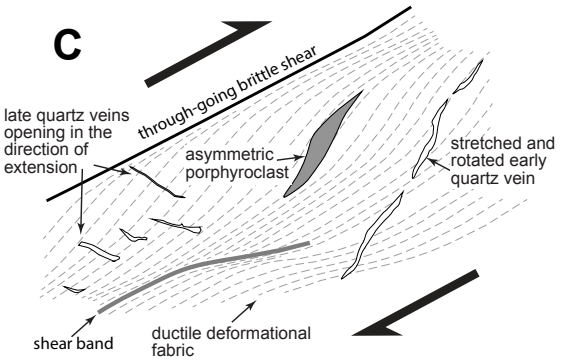

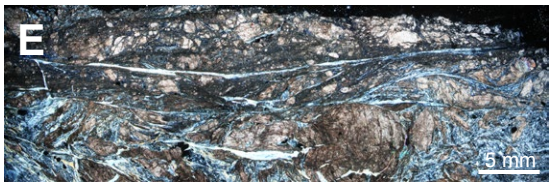

Figure 6. (A–C) Mixed-mode brittle-viscous deformation; (D–F) brittle structures. (A) Mode 1 quartz vein with columnar structure cutting a quartz shear vein formed along a thrust; the rock was subsequently deformed by dislocation creep and shows evidence for grain-boundary bulging and dynamic recrystallization. Later episodes of vein formation in the surrounding rock show that hydraulic fracture under low effective stress alternated with dislocation creep under high effective stress. Franciscan Complex, Middle Fork of the Eel River, northern California Coast Ranges (39.8294°N, 123.0700°W). Blueschist facies, 323 °C, 1.2 GPa (Schmidt and Platt, 2020). (B) Brittle and ductile structures within a major accretionary thrust (the Tomhead fault, 39.8529°N, 122.6957°W) in the Eastern belt of the Franciscan Complex, Thomes Creek, northern California Coast Ranges (Schmidt and Platt, 2018). The fault places blueschist-facies metabasalt (top left) above metachert (bottom right). Intense ductile deformation by dislocation creep is evidenced by the banding in the metasediments; note sigmoidal geometry center right (red star), indicating top-to-the-right shear sense. The rocks are cut by several generations of dilational quartz veins; older ones (at right, red arrow) have been rotated and stretched by ductile shear; younger ones (top left, blue arrow) are oriented normal to the extension direction in the shear zone. The combination of brittle and ductile deformation provides a mechanism for limiting displacement and displacement rate during individual slip events. Photos in A and B are by John Platt. (C) Schematic diagram illustrating the relationship of the structures in the shear zone shown in B to the overall sense of shear. (D) Discrete, serpentine-coated, slickensided fault surface from the Livingstone fault, New Zealand (from Tarling et al., 2019). 250–350 °C, 0.3–0.5 GPa. (E) Thin section photograph of a sample taken from D, showing multiple slip surfaces defined by fibrous serpentinite (see Tarling et al., 2019, their fig. 6). (F) Foliated chlorite slip surface on the margin of an altered basaltic block from the Mugi mélange, Shimanto accretionary complex, Japan. 190 °C (Kitamura et al., 2005; Phillips et al., 2020a). Photo is by Noah Phillips.

has led to a hypothesis that slow earthquakes are localized frictional events (e.g., Gao and Wang, 2017).

There are several hypotheses for how a frictional slip event might self-arrest or slow down to form a slow earthquake. These include rate dependence of rate-and-state friction parameters for specific geologic materials (i.e., materials that transition from velocity weakening to velocity strengthening with increasing slip velocity; e.g., Ikari et al., 2013; Im et al., 2020), blocks or regions of velocity-weakening material sitting near their critical nucleation lengths (Liu and Rice, 2007; Kotowski and Behr, 2019; Phillips et al., 2020a), or a reduction in pore-fluid pressure during slip due to dilation and/or fracturing (see previous section on veining). The following section reviews proposed geological signatures (and examples) for each of these mechanisms.

6.1 Coated Slip Surfaces and Phyllosilicate Horizons

These are localized slip surfaces that exhibit evidence of frictional slip (slickensides, slickenlines, polished surfaces) and may occur as localized layers within a wider zone of deformation, along the contacts of distinct lithologic units (where localization of deformation due to rheologic contrasts and/or chemical reactions is common), or as a thin surface in a foliated rock (e.g., a schist). Slip surfaces are frequently coated in phyllosilicate minerals (including talc, serpentine, and chlorite); these have a weak basal plane that facilitates frictional slip at stresses lower than that for most other rocks (Figs. 6D–6F). Coefficients of friction (the ratio of shear stress to normal stress required for sliding) for most phyllosilicate phases range from 0.1 to 0.4 (Behnsen and Faulkner, 2012), while coefficients of friction for most other minerals and rocks range from 0.7 to 0.8 (Byerlee, 1978).

Under low-temperature conditions (<~550 °C), chlorite-coated slip surfaces and chlorite-actinolite schists have been documented along the margins of mafic units and have been hypothesized to host slow earthquake phenomena (Fig. 6D; Phillips et al., 2020a; Tulley et al., 2022). Semicontinuous layers of altered basalt (which have elevated chlorite contents) are thought to exist along the upper margin of subducting slabs due to fluid-rock interactions along the plate interface, and blocks may be spalled into the surrounding metasediments. The breakdown of chlorite has been proposed as a mechanism to locally increase pore-fluid pressures, though this would only occur at specific temperatures along the plate interface (Tulley et al., 2022).

At greater depths, particularly in the region of the mantle wedge, metasomatic reactions between serpentinites and metasediments form localized serpentine and/or talc-rich layers. Tarling et al. (2019) documented localized serpentine slickenfibers and slickenlines within these reaction zones, which may represent slow earthquakes (Figs. 6D and 6E). These metasomatic reactions also produce fluids that may explain the observation of elevated pore-fluid pressures in the source regions of slow earthquake phenomena and that promote localized frictional slip. Frictional sliding in talc schist has been hypothesized to host slow earthquakes due to the extremely low coefficient of friction of talc (French and Condit, 2019), though field observations of talc-coated slip surfaces are rare. Recent observations by Hoover et al. (2022a) from Catalina Island indicated that talc-actinolite schists were deformed under higher-stress conditions than nearby chlorite-actinolite schists, which they interpreted as evidence that talc-schists accommodated greater strain rates through frictional sliding in the talc horizons (i.e., a potential slow earthquake).

Friction experiments on chlorite-rich lithologies (e.g., Ikari et al., 2013; Phillips et al., 2020b; Belzer and French, 2022) frequently exhibit a transition from velocity-weakening to velocity-strengthening behavior with increasing slip velocity, which has been proposed as a mechanism to produce slow earthquakes. Talc exhibits extremely low coefficients of friction (e.g., Moore and Rymer, 2007), and recent experiments at confining pressures >0.5 GPa indicate that talc exhibits coefficients of friction of ~0.01 at 700 °C, consistent with geophysical observations (e.g., Gao and Wang, 2017; Boneh et al., 2023). The rheology of serpentine is complex and cannot be fully summarized here (see reviews by Hirth and Guillot, 2013; Guillot et al., 2015), but experiments on serpentine have demonstrated that slow failure may occur under high pore-fluid pressure conditions (French and Zhu, 2017). In summary, while theoretical, experimental, and field observations indicate that frictional slip may host slow earthquakes, it is extremely difficult to definitively identify specific frictional features found in the field that formed at slow earthquake rates. Figure 7B, for example, shows a brittle fault zone with gouge fabric and Riedel shears cutting shale-matrix mélange in the Franciscan Complex in central California, but we have no basis for estimating the slip rate during deformation.

6.2 Block-in-Matrix Mélanges

Many exhumed subduction complexes contain block-in-matrix mélanges. These are characterized by relatively rigid blocks of various lithologies in a matrix, commonly either sheared mudstone or serpentinite (Figs. 7C–7E). Kotowski and Behr (2019) have described mélange consisting of fractured blocks of eclogite in ductilely deformed mafic blueschist (Fig. 7F), which would come under the heading of brittle-viscous behavior. The origin of these fragmental rocks is debated; some are clearly derived from sedimentary deposits, such as debris flows or olistostromes (Wakabayashi and Dilek, 2011; Platt, 2015); others are more likely to have a tectonic origin (e.g., Kimura et al., 2012; Kotowski and Behr, 2019). The presence of blocks of "exotic" rocks, such as basalt and chert in deformed graywacke matrix, and metamorphic rocks (blueschist, amphibolite, and eclogite) that are significantly higher grade than the matrix is commonly cited as an indicator of a tectonic origin, although these blocks can also be emplaced by surficial processes (Hitz and Wakabayashi, 2012; Platt, 2015). From the perspective of this article, the origin of the fragmental texture and the source of the blocks are not critical. The mechanical contrast between the blocks and the matrix, or a difference in their deformation mechanisms (brittle blocks vs. ductile matrix), has led to suggestions that these mixtures can lead to a combination of velocity-weakening behavior by fracture

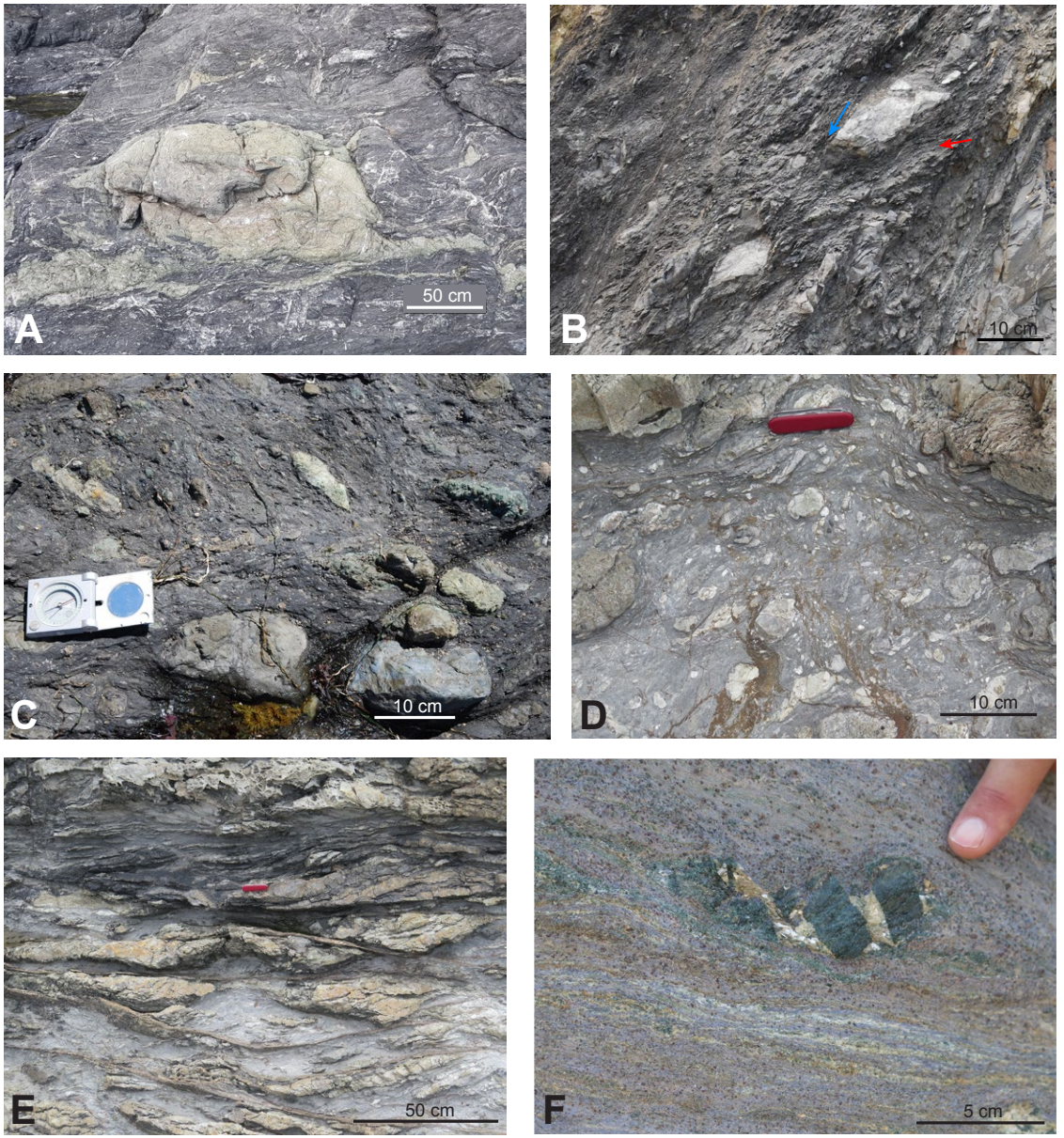

Figure 7. Block-in-matrix mélanges. (A) Basalt block with cataclasites developed along block margin within shale matrix, Upper Mugi mélange, Japan. 190 °C (Phillips et al., 2020a). (B) Brittle fault gouge in graywacke sandstone and shale, Franciscan Complex, Cayucos, California (35.4493°N, 120.9513°W) (Platt, 2015). This is an exhumation-related normal fault in rocks buried to ~15 km depth during Late Cretaceous subduction. Note disrupted quartz vein. Gouge fabric dips gently left (red arrow), and brittle shear bands dip more steeply left (blue arrow). The structures in this fault zone are characteristic of brittle faults formed in a wide variety of environments, and it is difficult to identify geologic signatures that could indicate they were responsible for slow earthquakes (cf. Fig. 6A). (C) Blocks of graywacke sandstone, blueschist (bottom right), and greenstone (top right) in scaly clay mélange, San Simeon, California (35.6008°N, 121.1344°W). 100–150 °C, 0.5 GPa (Ukar and Cloos, 2014). (D) Random fabric block-in-matrix mélange, Chrystalls beach, Otago, New Zealand (46.1897°S, 170.1155°E). <300 °C, 0.4–0.6 GPa (Fagereng et al., 2011). (E) Sheared block-in-matrix mélange, Chrystalls beach, Otago, New Zealand (46.1897°S, 170.1155°E). The shears are occupied by fiber-lineated quartz veins (see Fig. 5B). These structures were cited as a possible source of tremor and slow slip (Fagereng et al., 2011). (F) Eclogite blocks (green) in blueschist with dilational fractures, Kini beach, Syros, Greece, cited by Kotowski and Behr (2019) as a slow-slip signature. Photos in B–F are by John Platt.

or slip on the margins of the blocks and velocity-strengthening behavior by viscous flow of the matrix (Fagereng et al., 2014; Hayman and Lavier, 2014).

Block-and-matrix mélanges frequently occur as a wide (hundreds of meters to several kilometers) zone of deformation along the subduction plate interface (e.g., Rowe et al., 2013; Raimbourg et al., 2019; Tewksbury-Christle et al., 2021), and examples exhumed from conditions compatible with slow earthquakes are thought to correlate with low-velocity zones observed through geophysical methods (Tewksbury-Christle et al., 2021). The Shimanto accretionary complex in Japan allows for a detailed look at the changes in mélange style with depth along a subduction plate interface (Fig. 8). Differential exhumation produced a natural cross section through the accretionary prism at the surface, where peak pressure-temperature conditions during deformation increase from NE to SW. While much of the accretionary complex is composed of offscraped-turbidite sequences, several key exposures of the plate interface have been preserved through underplating and exhumation, allowing for structures formed from similar protoliths to be compared across a range of depths (Fig. 8). Typical block-in-matrix mélange fabrics from the Shimanto accretionary complex are shown in Figures 8B–8F. The mélanges are composed of blocks of metamorphosed sedimentary and basaltic igneous rocks within a shale matrix. Clast proportions and distributions vary substantially across individual mélange locations. Within the matrix, the intensity of pressure-solution fabrics increases with depth (Figs. 8C and 8E).

There are two main mechanistic models for producing slow earthquake phenomena in block-in-matrix mélanges. One treats mélange as a two-phase system with effectively rigid blocks in a viscous matrix and examines the effect of varying the block/matrix ratio or the distribution of blocks (Ando et al., 2010, 2023; Beall et al., 2019). Beall et al. (2019) demonstrated that if the block proportion is >50%, then blocks can jam up, giving the mélange as a whole a high strength. Fracture of the blocks can then lead to a drop in the bulk strength to a value close to that of the matrix. This could lead to cyclic behavior, with limited slow slip during the fracture events, accompanied by tremor, alternating with viscous flow. Ando et al. (2010) varied the distribution of blocks and demonstrated that a slow earthquake passing through sparsely distributed, brittle fault patches following a Gaussian distribution of size could produce low-frequency earthquakes with appropriate migration speeds and decay of source spectra.

The second class of models involves individual blocks (or block-rich horizons) sitting near their critical nucleation lengths for frictional failure to produce low-frequency earthquakes (e.g., Behr et al., 2021), which in the field is thought to represent the scale of blocks (or block-rich horizons). The critical nucleation length is the minimum length a rupture surface needs to produce dynamic slip (e.g., Uenishi and Rice, 2003; Rubin and Ampuero, 2005). In the case of mélanges, if blocks are too small, then brittle ruptures do not accelerate sufficiently to produce a measurable seismic signal; if they are too large, then ruptures will reach velocities sufficient to produce normal earthquakes rather than slow earthquakes. If blocks are sitting near their critical nucleation length, then a slow earthquake may occur. Critical nucleation lengths are strongly dependent on shear modulus, the rate of weakening, and the stress drop (which can be predicted using rate-and-state variables for the blocks and the normal stress acting across the fault). Critical nucleation lengths calculated for blocks at conditions of slow earthquakes range from tens of meters to several kilometers (Phillips et al., 2020a; Behr et al., 2021), with the large range due to variations in input parameters. At a larger scale, early numerical models produced slow-slip events using slightly velocity-weakening source regions to create very large critical slip distances (Liu and Rice, 2007).

In general, models predict that brittle failure of blocks, or frictional slip along block (or block train) margins, produces tremor events and low-frequency earthquakes, while concomitant distributed flow (through pressure-solution creep, dislocation creep, or cataclastic flow) in the matrix produces slow-slip events. In this theoretical framework, slow-slip events can both cause or be caused by failure of blocks. Several field studies have attempted to relate observed block sizes (and observations of brittle failure across blocks or coated slip surfaces along block margins) to specific slow earthquake phenomena (Kotowski and Behr, 2019; Phillips et al., 2020a), and block sizes exhibit a hierarchical (potentially power-law) distribution, which has been proposed as a mechanism for producing low-frequency earthquake size distributions (Fagereng, 2011; Frank and Brodsky, 2019; Kirkpatrick et al., 2021). Block-in-matrix mélanges are common along plate interfaces, and it is important to note that these models require near-lithostatic pore fluids to produce slow earthquakes, which may explain why slow earthquakes are not ubiquitous along plate interfaces (i.e., block-in-matrix mélanges do not necessarily produce slow earthquake phenomena). In examples where blocks and matrix both deform viscously by similar mechanisms, slow earthquakes are unlikely (e.g., De Caroli et al., 2024).

7. DISCUSSION

In the previous sections, we summarized three groupings for structures that may accommodate slow earthquakes and related phenomena. We now turn our attention to characteristics of slow earthquakes that might help to test hypotheses of possible structures. Critical questions we need to address include the consistency of proposed geological structures with the geophysical evidence for displacements, rates, and spatial and temporal scales of slow-slip phenomena. We examine the scaling relationships, whether geologic structures can reproduce the repeating behavior of low-frequency earthquakes, and whether they show the hierarchical structure of slow earthquakes. As an aid in this discussion, we summarize the possible position of the structures we discuss in the context of the seismic-aseismic transition in the subduction channel (Fig. 9).

7.1 Scaling Relationships

As discussed in Sections 3–6, there are many structures that could plausibly be associated with slow earthquakes, but these need to be evaluated not only

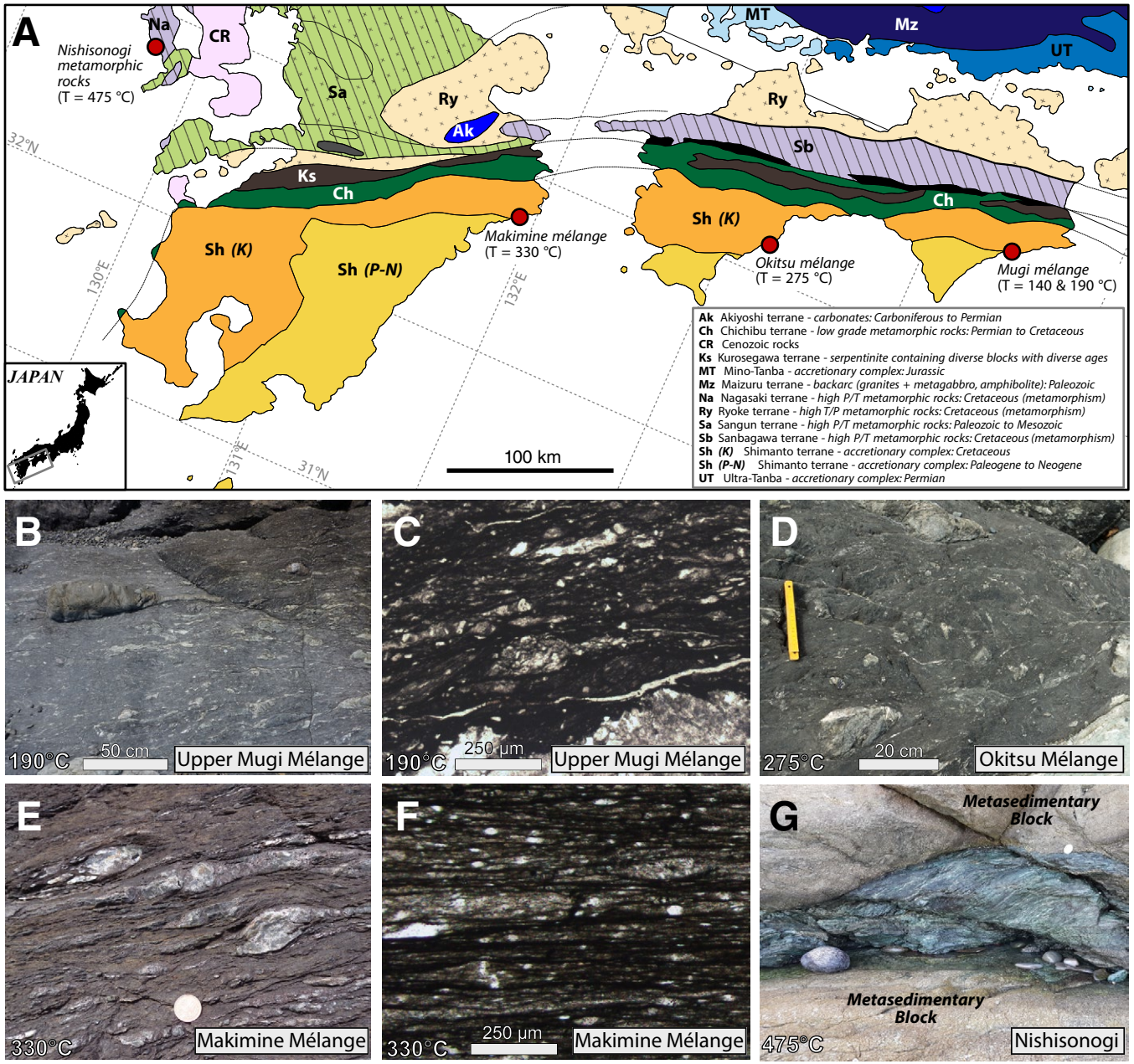

Figure 8. Examples of block-in-matrix mélanges (highlighting matrix fabrics) from exhumed subduction plate interfaces within the Shimanto accretionary complex and Nishisonogi metamorphic rocks of the Nagasaki terrane, Japan. (A) Summary map of the basement geology of Japan showing key outcrops of paleo–subduction plate interfaces and their temperatures of deformation (basement geology is after Wallis et al., 2020). Inset depicts location of geologic map (gray box). P/T—pressure/temperature. (B) Block-in-matrix fabrics from the Upper Mugi mélange. 190 °C. (C) Plane-polarized-light thin-section photomicrograph showing pressure-solution fabrics from the shale matrix of the Upper Mugi mélange. (D) Mélange fabrics from the Okitsu mélange. 275 °C. Photo courtesy of Dr. Arito Sakaguchi. (E) Block-in-matrix fabrics from the Makimine mélange. 330 °C. Photo by Chris Tulley (Tulley et al., 2022). (F) Plane-polarized-light thin-section photomicrograph of pressure-solution fabrics from the matrix of the Makimine mélange; note the increase in fabric intensity compared to C. (G) Two large (~5–10-m-diameter) folded metasedimentary rocks embedded in a fine-grained metabasalt (chlorite-actinolite schist) matrix from the Nishisonogi metamorphic rocks. 475 °C. Diameter of coin in E and G is 2 cm. Photos in B, C, F, and G are by Noah Phillips.

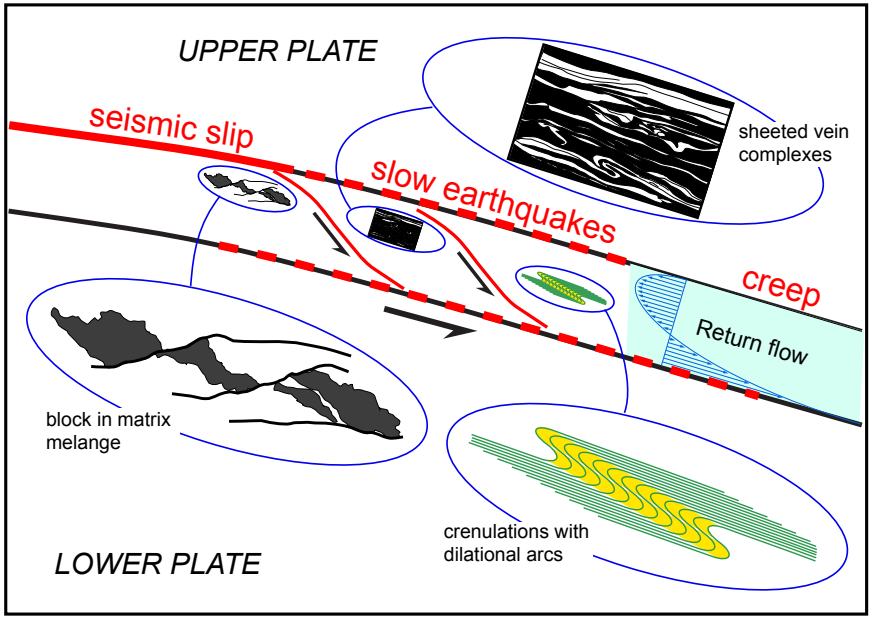

Figure 9. Schematic cross section of the transition zone in a subduction system showing the likely structural position of some of the structures discussed in this paper (not drawn to scale). Displacement in the transition zone becomes progressively more distributed downward through the subduction channel, due in part to underplating. Block-in-matrix mélanges involve mixed brittle and ductile shear, and in sedimentary materials, they are most likely to form within the seismic zone and the updip part of the transition zone. Sheeted vein complexes involve dilational shear and form in the transition zone. Both types of structures are likely to be associated with active slip surfaces. Crenulations with dilational arcs may form within a broad zone of ductile shear in the transition zone and may be associated with folding at scales from meters to kilometers; like sheeted vein complexes, they require fluid pressure approaching lithostatic.

in terms of their structural and rheological characteristics, but also in terms of their scaling relationships. Geophysical observations of slow earthquakes have constrained the relationships among total fault slip, duration, fault area, slip rate, seismic moment, and static stress drop (Ide et al., 2007a; Gao et al., 2012; Gomberg et al., 2016). The scaling relationships among these parameters provide a means to evaluate whether geological structures observed in the field could host slow earthquakes that are consistent with the geophysical observations. For example, the effective seismic moment M_{eff} can be calculated in the same way as for a normal earthquake, as $M_{eff} = sAG$, where s is the slip or displacement, A is the area of the deforming zone, and G is the shear modulus. In principle, s and A can be measured in the field, but we generally find that to produce a signal that can be detected remotely, A has to be larger than typical outcrops. G is well known for most rock-forming minerals, but it is much more poorly constrained, and probably much lower, for many rock types, particularly water-saturated sediments.

Low-frequency earthquakes provide a repeating finite source that might be correlated to structures at the outcrop scale. Several authors have used seismic recordings of low-frequency earthquakes to constrain the source parameters (Bostock et al., 2015; Thomas et al., 2016; Chestler and Creager, 2017). These studies suggest that an individual low-frequency earthquake may have a patch diameter of 200–600 m and experience 0.05–0.12 mm of fault slip per episode. This corresponds to a stress drop of 1–3 × 10^4 Pa. Additionally, several authors have suggested that the spatial dimensions of any given repeating low-frequency earthquake patch are generally constant, and changes in seismic moment release through time are mostly reflective of changes in slip amplitude per event (Bostock et al., 2015, 2017; Farge et al., 2020).

Chestler and Creager (2017) provided data for a low-frequency earthquake family near the updip limit of tremor within the Cascadia subduction zone beneath the Olympic Peninsula, Washington, northwestern United States. These tend to be larger families compared with those downdip. The total geodetic slip during slow slip events in this family during tremor events in 2010 and 2012 was 30 mm, assuming the slip was fully accommodated in one low-frequency earthquake patch. In total, 300 low-frequency earthquake events were detected, with a mean moment of 1.8 × 10^{11} Nm. Using the expression for effective seismic moment developed in the first paragraph of this section, with G = 30 GPa, the area of the tremor patch is 6 × 10^4 m^2, and hence it has a diameter of ~250 m. The authors assumed that the tremor patch consists of three subpatches that rupture fully during each low-frequency earthquake, based on their observations of where the low-frequency earthquake families mapped within a patch, and they assumed a total slip per low-frequency earthquake = 0.5 mm, with a range of 0.1–1 mm.

The implication of these data is that a geophysically detectable low-frequency earthquake source needs to have a displacement of 0.1–1 mm and a linear dimension of ~300 m. The displacement should take place in ~1 s, which implies slip rates in the range 10^{-3} m/s to 10^{-4} m/s. The incremental displacements inferred from vein widths, crack-seal increments, and the size of structures, such as dilational crenulation arcs, are on the order of a few tens

of micrometers to ~1 mm, and they are therefore very similar in magnitude to low-frequency earthquake slip magnitudes (Behr and Bürgmann, 2021). The durations of slip events (and hence the slip rate) are much more difficult to estimate from geological evidence. Individual frictional slip surfaces record the total slip accommodated by that surface, and it is difficult to constrain the number of slip events, the offset during a single event, or the rate of slip. Rates of shear strain in ductile shear zones can be estimated (with significant uncertainty) using a combination of dynamically recrystallized grain-size paleopiezometry and experimentally established flow laws (e.g., Behr and Platt, 2011, 2013; Boutonnet et al., 2013; Xia and Platt, 2017; Lusk and Platt, 2020). Unless a very clear relationship can be established between ductile strain rates and slip rates on discrete fractures, however, this does not provide a clear basis for comparison with geophysical data from slow earthquakes.

7.2 Repeating Structures

A characteristic feature of low-frequency earthquakes is their repetitive nature; each low-frequency earthquake source generates many events in time, called multiplets (Sweet et al., 2014; Frank et al., 2014). Given the same source, path, and recording station, each low-frequency earthquake multiplet from a single source is characterized by similar waveforms. Given that low-frequency earthquakes are distinct slow earthquake phenomena that are most likely to correlate with structures observable at the outcrop scale, we need to search for structures with regularly spaced geometries, or structures with a strain-insensitive geometry, that can produce repeating events. Possibilities include folds and boudins, en échelon or regularly spaced fractures, sheeted vein complexes, crack-seal structures within veins, and discrete slip surfaces. The time required for healing of dilational fractures such as crack-seal structures with displacements of 1 mm or less can range from a few hours (Smith and Evans, 1984; Brantley et al., 1990; Brantley, 1992) to a few days (Fisher and Brantley, 2014), which is compatible with the repeat times of low-frequency earthquakes.

Small-scale folds and boudins are structures with a scale controlled by the thickness and viscosity contrast of bedding in sedimentary rocks (Biot, 1961; Smith, 1977). Accretionary complexes are commonly dominated by sequences of alternating sandstones and shales deposited by turbidity currents, with regular bedding thicknesses in the range 1–100 cm, which may show trains of folds or boudins with dimensions controlled by the bedding. Folding and boudinage at low temperature may involve both fracture or frictional sliding and viscous flow. Folding commonly involves a component of bedding-parallel slip on the limbs of the folds (flexural slip) and extensional fracturing on the outer arcs of buckle folds, and boudinage commonly leads to regularly spaced ruptures of an extended layer. These structures are analogous to viscous shear zones, in that the displacement and displacement rate are distributed across the structure, and they have to be calculated from the strain rate and the width of the structure. Their characteristics are consistent with the possibility that they are the source of repeating low-frequency earthquakes, but we are not able to constrain the strain rate (and hence displacement rate) or the propagation velocity precisely enough to be diagnostic.

At a smaller scale, foliated rocks produced by ductile deformation can produce microfolds during a second or subsequent phase of deformation, and if fluid pressures are high, microfold arcs may become the locus of dilational fractures, as discussed in Section 4.4. Repeated dilational fracturing may be required to enable enough fluid to pass through these arcs to precipitate the quartz that eventually fills them, and this repeated fracturing of the same geometrical structure provides a potential mechanism to explain repeating low-frequency earthquakes.

Sheeted vein complexes (discussed in Section 4) appear to involve repetitive dilational fracture to produce closely spaced veins of similar thickness and lateral extent. Their spacing is likely to be controlled by the length of the fractures and the elastic properties of the surrounding rock (Bai and Pollard, 2000; Bonnet et al., 2019; Van Noten and Sintubin, 2010), though the controls on spacing of mode 1 and mode 2 veins may be very different. Given that sheeted shear veins (mode 2) are among the most plausible sources of slow earthquakes, further research is needed to better understand their repetitive character.

Crack-seal structures (discussed in Sections 4.1 and 4.2) involve repetitive fracture within veins. These commonly show very consistent spacings within individual veins, reflecting consistent mechanical controls on the hydraulic fracture process. The most likely cause of this is cyclic variations in pore-fluid pressure, and hence effective normal stress, controlled by the permeability of the surrounding rock. The consistent spacing suggests that a single shear surface is able to produce slip events that repeat hundreds to thousands of times with a "characteristic" displacement (Fagereng et al., 2011). The implication of this observation is that the slip rate may be controlled by steady-state creep in the matrix rather than by the properties of the slip surface itself. Crack-seal structures are the most suitable structures for unambiguously linking growth increments in shear veins to phases of fault slip (Roberts and Holdsworth, 2022).

Discrete slip surfaces may be capable of producing repeating low-frequency earthquakes, as shown by repeating microearthquakes or "repeaters" (see review by Uchida and Bürgmann, 2019, and references within). These are small (generally $M < 4$) "normal" earthquakes that show similar waveforms (e.g., Geller and Mueller, 1980; Vidale et al., 1994; Uchida and Bürgmann, 2019). The process of identifying repeaters is similar to that for low-frequency earthquakes; they are frequently identified based on identical hypocenter locations and waveform similarity (i.e., high cross-correlation coefficients) and are interpreted to represent repeated failure of the same fault patch. Similar repeated failure of discrete slip surfaces with appropriate frictional properties (see Section 6) could produce repeating low-frequency earthquakes. Evidence for repeated slip events on individual slip surfaces has been documented where individual frictional slip surfaces variably offset multiple generations of mode 1 veins (e.g., Phillips et al., 2020a).

7.3 Hierarchical Structures

Another distinctive characteristic of slow earthquakes is their hierarchical nature. Low-frequency earthquakes typically last a few seconds, but they form a constituent part of tremor bursts, which accompany transient slow-slip events lasting days to weeks. These slow transients in turn build up longer-duration and larger-moment slow-slip events lasting months as the event propagates (Frank et al., 2018). This corresponds to a range in linear dimension for the source region of slow earthquakes of ~4 orders of magnitude, a similar range in displacement, and a range in equivalent seismic moment of ~9 orders of magnitude. The relationship across scales suggests that part of the displacement in slow-slip events is achieved by the displacements accumulated by the low-frequency earthquakes. If true, we can understand a lot about what is happening in rocks during slow-slip events by looking at structures representing low-frequency earthquakes. We should bear in mind, however, that only a small fraction of the moment magnitude is associated with the family of seismic emissions (tremor, low-frequency earthquakes, very low-frequency earthquakes; Frank and Brodsky, 2019). In this regard, seismic slip is a minor process in the slow-slip region, but it appears to be scattered throughout the zone. Some patches produce some seismic waves, but the majority of the fault surface (or volume) experiences aseismic slip on the fault or distributed viscous deformation in the volume.

The hierarchical relationship among slow earthquakes at different scales suggests that we need to search for sets of structures that have a comparable hierarchical character in terms of linear dimension and displacement, bearing in mind that slip rates and strain rates are much more difficult to constrain from geological evidence. An example of such a hierarchical set of structures is provided by folds. It has long been recognized that small-scale folds contribute to the strain involved in the development of larger-scale folds with related geometry over wide ranges of scale. Similarly, in strongly foliated rocks, microfolds or crenulations accompanied by solution-redeposition creep may be responsible for substantial strain, and they contribute to the development of meter-scale folds, forming an axial-plane cleavage. Meter-scale folds in turn accompany the development of larger-scale structures, up to the kilometer scale. These structures have ranges in both linear dimension and displacement of at least 4 orders of magnitude, and they provide a close analogy to the seismically and geodetically observed hierarchy of slow earthquakes.

Could different scales of folding be responsible for different scales of slow earthquakes? In most metamorphic terranes, folding is achieved by ductile deformational processes such as solution-precipitation creep or dislocation creep, which operate at rates that are orders of magnitude too slow to produce slow-slip events. As described in Section 4.3, however, crenulations in parts of the Franciscan Complex were accompanied by dilational cracking in the crenulation arcs. The rate of opening of these fluid-filled arcs, and the rate of propagation of the crenulation bands, could have happened at rates compatible with low-frequency earthquakes. The arcs were subsequently filled with quartz, probably by diffusion of silica, at rates far slower than the time scales of slow earthquakes. Dilational cracking and propagation of linked sets of crenulation bands could lead to the incremental amplification of folds on different scales, with each such increment leading to a slow-slip event accompanied by tremor bursts and low-frequency earthquakes.

Some types of veins are hierarchical, in that larger veins appear to be constructed of small-scale crack-seal events, and sheeted vein complexes are built from successive dilational fractures. The range of displacement for mode 1 veins and vein complexes is therefore ~5 orders in magnitude, and it may be larger for shear veins; the range in linear dimension in the plane of the veins is more difficult to determine due to outcrop constraints, but it may be ~3 orders of magnitude. Brittle and brittle-viscous shear zones do not obviously exhibit hierarchical character; large shear zones are not made up of a lot of smaller ones, although they may incorporate a subset of smaller-scale shear bands or Riedel shears.

The size of blocks in block-in-matrix fabrics shows a power-law (fractal) distribution (Fagereng, 2011), although the fractal dimension is variable, and this has been compared to the scale-invariant character of faults and normal earthquakes (Kirkpatrick et al., 2021). Block-in-matrix fabrics do not show hierarchical character, however; large blocks are not aggregates of smaller blocks. The relationship between the block-in-matrix fabrics and different scales of slow earthquakes is likely to be different: The power-law distribution of the blocks may produce variable-sized low-frequency earthquakes, while distributed flow in the matrix may produce longer-period slow-slip events (e.g., Behr et al., 2021; Kirkpatrick et al., 2021). Alternatively, numerical simulations by Barbot (2019) suggest that rupture processes can unfold at different length scales simultaneously, allowing both widespread slow slip and localized slow earthquakes unrelated to the scale of structural heterogeneities.

7.4 Summary

Table 1 summarizes the conclusions of the discussion here, in terms of how well the various structures we have described fit the requirements to produce low-frequency earthquakes and the characteristics of the slow earthquake family. The structures that seem to fit best are shear veins and crenulations with dilational arcs. Mode 1 veins appear to be disqualified because they do not show shear displacement, which is indicated by focal mechanism analysis of low-frequency earthquakes, but they may contribute to the overall tremor signal, particularly if they occur within larger-scale shear zones (e.g., the en échelon vein sets illustrated in Fig. 4E). In brittle-viscous shear zones, the viscous component of deformation can limit the displacement and displacement rate during slow earthquakes, and this process may potentially scale up to geodetically observable slow-slip events. As discussed in Section 6, in purely brittle shear zones, processes that could limit displacement and displacement rate include the presence of specific geologic materials that transition from velocity-weakening to velocity-strengthening behavior with increasing slip velocity, blocks or regions of velocity-weakening material sitting near their

TABLE 1. CHARACTERISTICS OF CANDIDATE STRUCTURES FOR GENERATING SLOW EARTHQUAKES

	Displacement	Shear	Limits	Length scale	Repeating	Hierarchy
Mode 1 veins	10^{-5} to 10^{-3} m	No	Yes	1–10^{3} m?	Yes	Yes
Shear veins	10^{-5} to 10^{-3} m	Yes	Yes	1–10^{3} m?	Yes	Yes
Dilational microfold arcs	10^{-4} to 10^{-3} m	Yes	Yes	1–10^{3} m	Yes	Yes
Brittle-viscous shear zones	No constraints	Yes	Yes	No constraints	No	No
Brittle shear zones	A few centimeters?	Yes	Yes	1–10^{3} m	Yes	No
Block-in-matrix	A few centimeters?	Yes	Yes	10^{-1}–10^{3} m	No	No

Notes: Displacement refers to the maximum incremental displacement in individual events. Shear refers to whether or not the dominant displacement lies within the plane of the structure. Limits refers to whether there are inherent limits on the displacement, rate of displacement, or both. Length-scale refers to the dimension in the plane of the structure. For brittle and brittle-viscous shear zones, these depend on whether the geometry or mechanical properties lead to velocity or strain-rate hardening behavior. See discussion in the text.

critical nucleation lengths, and dilational hardening. Brittle-viscous shear zones and block-in-matrix mélanges do not show a clearly identifiable mechanism for producing repeating events, but brittle shear zones may contain asperities that fail repeatedly in this way. Brittle shear zones, brittle-viscous shear zones, and block-in-matrix mélanges lack the hierarchical character of slow earthquakes across a range of spatial scales. Whether these conclusions will hold up depends on the outcomes of future research, which we discuss in the next section.

8. TARGETS FOR FUTURE RESEARCH

Future research efforts should focus on a range of topics that would help to discern more precisely the geological structures that host slow earthquakes. An expanded suite of laboratory friction experiments would greatly assist field geologists in interpreting the fingerprints of slow earthquakes. A better characterization of microstructures from these experiments is needed for more detailed comparison to microstructures from natural samples. Future experiments should intently focus on the frictional behavior of materials that are conditionally stable under conditions of high pore-fluid pressure, as this regime allows frictional sliding to move seamlessly between two modes of deformation. Experiments involving repeated frictional events would be particularly interesting and instructive. Additionally, the elasto-plastic behavior of rocks is understudied and may prove to be crucial in better understanding the mixed-mode response of rocks under strain. As always, the scaling of fault properties (e.g., spatial dimensions, roughness) from the laboratory to the field remains a challenge; the development of nondimensional parameters may help to better connect laboratory and field observations (e.g., Barbot, 2019).

New progress in geochemical and petrological techniques may contribute to new insights. Fluid-rock interactions are pervasive at the depths and temperatures of slow earthquakes. Work over the last decade on fluid-rock interactions has shown that reactions involving fluids may occur very rapidly (e.g., Putnis 2009), so that structures involving localized reactions, such as replacement veins (Bons et al. 2012), may be of particular interest. New geochemical tracers and isotopic techniques, such as Li isotopes (e.g., Hoover et al., 2022b), are critical for tracking where fluids are coming from in the plate-boundary system as well as the duration of fluid flow (e.g., Taetz et al., 2018). This can help to discern whether fluids are produced locally in the rock versus being advected from elsewhere in the subduction-zone system (e.g., Penniston-Dorland et al., 2012; Taetz et al., 2016; Nishiyama et al., 2020). New constraints on mineral precipitation rates would refine time scales for crack sealing and improve our understanding of the kinetics and cyclicity of deformation. Studies of deformational structures need to be combined with in-depth analysis of the pressure, temperature, and fluid conditions at which deformation occurred, allowing linkage of deformation to metamorphic reactions that contribute to bulk-rock weakening and changes in fluid pressure. It may also be possible to derive rates of short-term events using chemical diffusion modeling.

Numerical models will be critical for testing hypotheses based on field observations. These models are highly dependent on the permeability structure of shear zones, which is best informed by field observations (Muñoz-Montecinos and Behr, 2023). Numerical simulations need realistic estimates of bulk permeability to accurately replicate the mechanics. Brittle-ductile shear zone systems are likely to be very heterogeneous (e.g., material properties, friction and cohesion, fluid pressure, microstructure). Geologists need to better characterize the amplitude and scale of each of these heterogeneities in the field. New ideas on how force chains and patterns of granular flow, which naturally result in stress heterogeneities, may reveal complex deformation patterns in shear zones. The resulting microstructures might allow mapping of stress heterogeneities related to transient viscous deformation. The identification of structures produced by stress concentrations in the field, using high-resolution field mapping aided by cutting-edge technologies (e.g., drones) coupled with systematic microstructural analyses, may also help to indicate where and how transient deformation first nucleates.

There is a range of additional field observations that could further aid in our understanding of slow earthquakes, and some of these may best be carried out in exhumed strike-slip zones, such as the Alpine fault in New Zealand, where the structures are arguably less affected by exhumation-related deformation. Given that near-lithostatic pore pressure has been inferred for slow earthquakes, one would expect hydraulic fracturing to be a calling card in

the rock record, yet field observations find veins in some areas but not others. A key observation that is needed is documentation of the orientation of veins relative to the direction of shear within the broader deforming zone, as this may provide a tight constraint on the relative state of stress. The current geophysical data sets provide poor constraints on the thicknesses of deforming zones at depth. We need better geological descriptions of the thicknesses of the shear zones, both those that describe individual slip episodes as well as broader zones that host repeated evolving deformation cycles.

In summary, while much work has been done to characterize potential geological structures associated with slow earthquakes, there are still many outstanding questions and avenues for future research. Most of these require close interdisciplinary collaborations among the field research, experimental rock deformation, geochemistry, geochronology, and geophysics communities.

9. CONCLUSIONS

The analysis presented in this paper allows us to define a number of considerations that can help in identifying evidence of slow earthquakes in the geological record:

(1) Slow earthquakes have so far mainly been identified from active subduction zones around the Pacific Rim, many of which are heavily sedimented, and from a small number of continental transform boundaries. Most (but not all) such phenomena are identified at depths of 40–60 km in subduction zones. The geological fingerprints of these processes are therefore best searched for in rocks exhumed from these depths in active and ancient accretionary complexes.

(2) Various candidate structures have been identified that could host slow earthquakes, and it is unlikely that there is one universal structure that explains all of the geophysical observations. Rather, there is likely a collection of structures and mechanisms that produce macroscopically observed slow earthquake phenomena.

(3) Collectively, slow earthquake phenomena (including transient aseismic slip, tremor events, and low-frequency earthquakes) require the simultaneous action of a brittle process acting at close-to-seismic rates and a quasi-viscous process that limits both the displacement and the rate of displacement.

(4) The high pore-fluid pressures inferred from shear wave velocities and Vp/Vs ratios in subduction zones suggest that structures related to slow-slip events are likely to be associated with hydraulic fractures (e.g., veins) and with metamorphic reactions that release or consume water.

(5) Loss of continuity, and resulting slip at rates exceeding 10^{-4} m/s, is required to produce the quasi-seismic signature of low-frequency earthquakes. The displacement associated with a single low-frequency earthquake is unlikely to exceed ~1 mm; otherwise, slip is likely to accelerate to the point of producing a normal earthquake. Displacements <0.1 mm are unlikely to produce sufficient seismic moment. Subseismic displacement rates during low-frequency earthquakes may result if the slip rate is slowed by a viscous dashpot, such as low permeability limiting the rate at which fluid can access a propagating fracture or viscous flow in the surrounding rock. The lateral extent of the displacement surfaces has to be on the order of a few hundred meters to produce sufficient seismic moment.

(6) Structures that can produce repeated small displacements, or sets of structures with similar geometry and mechanical properties, are required to explain repeating low-frequency earthquakes.

(7) Structural hierarchies, where displacements on smaller structures contribute to the development of the larger structures, are required to explain the hierarchies of slow-slip events (e.g., low-frequency earthquakes, tremor bursts, geodetically detectable slow-slip events).

Structures that may meet some or all of these criteria include:

(1) Sheeted vein complexes. Mode 1 veins (which open normal to the vein surface) may not qualify, as the seismic evidence suggests that low-frequency earthquakes represent double-couple shear events. Mode 2 (shear) veins qualify on these grounds and fulfill most of the other criteria.

(2) Regularly spaced veins, such as en échelon vein sets in shear zones. Although these veins are mode 1 fractures, the fact that they form in a shear zone may mean that they can produce a double-couple shear signal.

(3) Dilational arcs in microfold hinges that contribute to crenulation cleavage bands, and to the amplification of medium- to large-scale folds.

(4) Brittle-ductile shear zones, where the viscous component of deformation can limit the displacement rate during slow-slip events.

(5) Slip surfaces coated with materials such as chlorite or serpentine that exhibit a transition from velocity-weakening to velocity-strengthening behavior.

(6) Block-in-matrix mélanges with large blocks or block-rich horizons (100 m to kilometers in scale) in a viscous or quasi-viscous matrix, such that fracturing of the blocks can produce a high-slip-rate event, but the displacement and displacement rate are limited by quasi-viscous flow in the matrix.

ACKNOWLEDGMENTS

This work was motivated by discussions at a Penrose Conference funded by the Geological Society of America, the National Science Foundation (EAR-2025105), and the Southern California Earthquake Center (SCEC-19133). We thank the many participants in the conference whose contributions informed the discussions in this paper. We appreciate detailed and constructive reviews by Simon Peacock, Francesca Meneghini, and an anonymous reviewer, and editorial management by Associate Editor Francesco Mazzarini, all of which contributed substantially to improving the manuscript.

REFERENCES CITED

Ando, R., Nakata, R., and Hori, T., 2010, A slip pulse model with fault heterogeneity for low-frequency earthquakes and tremor along plate interfaces: Geophysical Research Letters, v. 37, no. 10, L10310, https://doi.org/10.1029/2010GL043056.

Ando, R., Ujiie, K., Nishiyama, N., and Mori, Y., 2023, Depth-dependent slow earthquakes controlled by temperature dependence of brittle-ductile transitional rheology: Geophysical Research Letters, v. 50, https://doi.org/10.1029/2022GL101388.

Andreani, M., Baronnet, A., Boullier, A.M., and Gratier, J.P., 2004, A microstructural study of a "crack-seal" type serpentine vein using SEM and TEM techniques: European Journal of Mineralogy, v. 16, p. 585–595, https://doi.org/10.1127/0935-1221/2004/0016-0585.

Audet, P., and Bürgmann, R., 2014, Possible control of subduction zone slow-earthquake periodicity by silica enrichment: Nature, v. 510, p. 389–392, https://doi.org/10.1038/nature13391.

Audet, P., and Kim, Y., 2016, Teleseismic constraints on the geological environment of deep episodic slow earthquakes in subduction zone forearcs: A review: Tectonophysics, v. 670, p. 1–15, https://doi.org/10.1016/j.tecto.2016.01.005.

Audet, P., and Schaeffer, A.J., 2018, Fluid pressure and shear zone development over the locked to slow slip region in Cascadia: Science Advances, v. 4, https://doi.org/10.1126/sciadv.aar2982.

Audet, P., Bostock, M.G., Christensen, N.I., and Peacock, S.M., 2009, Seismic evidence for overpressured subducted oceanic crust and megathrust fault sealing: Nature, v. 457, p. 76–78, https://doi.org/10.1038/nature07650.

Baba, S., Obara, K., Takemura, S., Takeo, A., and Abers, G.A., 2021, Shallow slow earthquake episodes near the trench axis off Costa Rica: Journal of Geophysical Research: Solid Earth, v. 126, https://doi.org/10.1029/2021JB021706.

Bai, T., and Pollard, D.D., 2000, Fracture spacing in layered rocks: A new explanation based on the stress transition: Journal of Structural Geology, v. 22, p. 43–57, https://doi.org/10.1016/S0191-8141(99)00137-6.

Baratin, L.-M., Chamberlain, C.J., Townend, J., and Savage, M.K., 2018, Focal mechanisms and inter-event times of low-frequency earthquakes reveal quasi-continuous deformation and triggered slow slip on the deep Alpine fault: Earth and Planetary Science Letters, v. 484, p. 111–123, https://doi.org/10.1016/j.epsl.2017.12.021.

Barbot, S., 2019, Slow-slip, slow earthquakes, period-two cycles, full and partial ruptures, and deterministic chaos in a single asperity fault: Tectonophysics, v. 768, https://doi.org/10.1016/j.tecto.2019.228171.

Bartlow, N.M., 2020, A long-term view of episodic tremor and slip in Cascadia: Geophysical Research Letters, v. 47, https://doi.org/10.1029/2019GL085303.

Beach, A., 1975, The geometry of en-echelon vein arrays: Tectonophysics, v. 28, p. 245–263, https://doi.org/10.1016/0040-1951(75)90040-2.

Beall, A., Fagereng, Å., and Ellis, S., 2019, Strength of strained two-phase mixtures: Application to rapid creep and stress amplification in subduction zone mélange: Geophysical Research Letters, v. 46, no. 1, p. 169–178, https://doi.org/10.1029/2018GL081252.

Behnsen, J., and Faulkner, D.R., 2012, The effect of mineralogy and effective normal stress on frictional strength of sheet silicates: Journal of Structural Geology, v. 42, p. 49–61, https://doi.org/10.1016/j.jsg.2012.06.015.

Behr, W.M., and Bürgmann, R., 2021, What's down there? The structures, materials and environment of deep-seated slow slip and tremor: Philosophical Transactions of the Royal Society, A: Mathematical, Physical, and Engineering Sciences, v. 379, no. 2193, https://doi.org/10.1098/rsta.2020.0218.

Behr, W.M., and Platt, J.P., 2011, A naturally constrained stress profile through the middle crust in an extensional terrane: Earth and Planetary Science Letters, v. 303, p. 181–192, https://doi.org/10.1016/j.epsl.2010.11.044.

Behr, W.M., and Platt, J.P., 2013, Rheological evolution of a Mediterranean subduction complex: Journal of Structural Geology, v. 54, p. 136–155, https://doi.org/10.1016/j.jsg.2013.07.012.

Behr, W.M., and Platt, J.P., 2014, Brittle faults are weak, yet the ductile middle crust is strong: Implications for lithospheric mechanics: Geophysical Research Letters, v. 41, p. 8067–8075, https://doi.org/10.1002/2014GL061349.

Behr, W.M., Gerya, T.V., Cannizzaro, C., and Blass, R., 2021, Transient slow slip characteristics of frictional-viscous subduction megathrust shear zones: AGU Advances, v. 2, https://doi.org/10.1029/2021AV000416.

Belzer, B.D., and French, M.E., 2022, Frictional constitutive behavior of chlorite at low shearing rates and hydrothermal conditions: Tectonophysics, v. 837, https://doi.org/10.1016/j.tecto.2022.229435.

Beroza, G.C., and Ide, S., 2011, Slow earthquakes and nonvolcanic tremor: Annual Review of Earth and Planetary Sciences, v. 39, p. 271–296, https://doi.org/10.1146/annurev-earth-040809-152531.

Biot, M.A., 1961, Theory of folding of stratified viscoelastic media and its implications in tectonics and orogenesis: Geological Society of America Bulletin, v. 72, p. 1595–1620, https://doi.org/10.1130/0016-7606(1961)72[1595:TOFOSV]2.0.CO;2.

Boneh, Y., Pec, M., and Hirth, G., 2023, High-pressure mechanical properties of talc: Implications for fault strength and slip processes: Journal of Geophysical Research: Solid Earth, v. 128, https://doi.org/10.1029/2022JB025815.

Bonnet, G., Agard, P., Angiboust, S., Fournier, M., and Omrani, J., 2019, No large earthquakes in fully exposed subducted seamount: Geology, v. 47, p. 407–410, https://doi.org/10.1130/G45564.1.

Bons, P.D., Elburg, M.A., and Gomez-Rivas, E., 2012, A review of the formation of tectonic veins and their microstructures: Journal of Structural Geology, v. 43, p. 33–62, https://doi.org/10.1016/j.jsg.2012.07.005.

Bostock, M.G., Thomas, A.M., Savard, G., Chuang, L., and Rubin, A.M., 2015, Magnitudes and moment-duration scaling of low-frequency earthquakes beneath southern Vancouver Island: Journal of Geophysical Research: Solid Earth, v. 120, no. 9, p. 6329–6350, https://doi.org/10.1002/2015JB012195.

Bostock, M.G., Thomas, A.M., Rubin, A.M., and Christensen, N.I., 2017, On corner frequencies, attenuation, and low-frequency earthquakes: Journal of Geophysical Research: Solid Earth, v. 122, p. 543–557, https://doi.org/10.1002/2016JB013405.

Boutonnet, E., Leloup, P.H., Sassier, C., Gardien, V., and Ricard, Y., 2013, Ductile strain rate measurements document long-term strain localization in the continental crust: Geology, v. 41, p. 819–822, https://doi.org/10.1130/G33723.1.

Brantley, S.L., 1992, The effect of fluid chemistry on quartz microcrack lifetimes: Earth and Planetary Science Letters, v. 113, p. 145–156, https://doi.org/10.1016/0012-821X(92)90216-I.

Brantley, S.L., Evans, B., Hickman, S.H., and Crerar, D.A., 1990, Healing of microcracks in quartz: Implications for fluid flow: Geology, v. 18, p. 136–139, https://doi.org/10.1130/0091-7613(1990)018<0136:HOMIQI>2.3.CO;2.

Brodie, K.H., and Rutter, E.H., 1987, The role of transiently fine-grained reaction products in syntectonic metamorphism: Natural and experimental examples: Canadian Journal of Earth Sciences, v. 24, p. 556–564, https://doi.org/10.1139/e87-054.

Byerlee, J., 1978, Friction of rocks: Pure and Applied Geophysics, v. 116, p. 615–626, https://doi.org/10.1007/BF00876528.

Calvert, A.J., Bostock, M.G., Savard, G., and Unsworth, M.J., 2020, Cascadia low frequency earthquakes at the base of an overpressured subduction shear zone: Nature Communications, v. 11, 3874, https://doi.org/10.1038/s41467-020-17609-3.

Caputo, R., and Hancock, P.L., 1999, Crackjump mechanism and its implications for stress cyclicity during extension fracturing: Journal of Geodynamics, v. 27, p. 45–60, https://doi.org/10.1016/S0264-3707(97)00029-X.

Cerchiari, A., Remitti, F., Mittempergher, S., Festa, A., Lugli, F., and Cipriani, A., 2020, Cyclical variations of fluid sources and stress state in a shallow megathrust-zone mélange: Journal of the Geological Society, v. 177, p. 647–659, https://doi.org/10.1144/jgs2019-072.

Chapman, T., Milan, L., and Vry, J., 2022, The role of metamorphic fluid in tectonic tremor along the Alpine fault, New Zealand: Geophysical Research Letters, v. 49, https://doi.org/10.1029/2021GL096415.

Chen, J., 2023, The emergence of four types of slow slip cycles on dilatant, fluid saturated faults: Journal of Geophysical Research: Solid Earth, v. 128, https://doi.org/10.1029/2022JB024382.

Chestler, S.R., and Creager, K.C., 2017, Evidence for a scale-limited low-frequency earthquake source process: Journal of Geophysical Research: Solid Earth, v. 122, no. 4, p. 3099–3114, https://doi.org/10.1002/2016JB013717.

Condit, C.B., and French, M.E., 2022, Geologic evidence of lithostatic pore fluid pressures at the base of the subduction seismogenic zone: Geophysical Research Letters, v. 49, no. 12, https://doi.org/10.1029/2022GL098862.

Condit, C.B., Guevara, V.E., Delph, J.R., and French, M.E., 2020, Slab dehydration in warm subduction zones at depths of episodic slip and tremor: Earth and Planetary Science Letters, v. 552, https://doi.org/10.1016/j.epsl.2020.116601.

Cox, S.F., and Etheridge, M.A., 1983, Crack-seal fibre growth mechanisms and their significance in the development of oriented layer silicate microstructures: Tectonophysics, v. 92, p. 147–170, https://doi.org/10.1016/0040-1951(83)90088-4.

De Caroli, S., Fagereng, Å., Ujiie, K., Blenkinsop, T., Meneghini, F., and Muir, D., 2024, Deformation microstructures of low- and high-strain epidote-blueschist (Ryukyu arc, Japan): Implications for subduction interface rheology: Journal of Structural Geology, v. 180, https://doi.org/10.1016/j.jsg.2023.105041.

Dragert, H., Wang, K., and James, T.S., 2001, A silent slip event on the deeper Cascadia subduction interface: Science, v. 292, no. 5521, p. 1525–1528, https://doi.org/10.1126/science.1060152.

Dumitru, T., Wakabayashi, J., Wright, J.E., and Wooden, J.L., 2010, Early Cretaceous (ca. 123 Ma) transition from nonaccretionary behavior to strongly accretionary behavior within the Franciscan subduction complex: Tectonics, v. 29, TC5001, https://doi.org/10.1029/2009TC002542.

Fagereng, Å., 2011, Frequency-size distribution of competent lenses in a block-in-matrix mélange: Imposed length scales of brittle deformation?: Journal of Geophysical Research: Solid Earth, v. 116, no. B5, B05302, https://doi.org/10.1029/2010JB007775.
Fagereng, Å., and den Hartog, S.A.M., 2016, Subduction megathrust creep governed by pressure solution and frictional-viscous flow: Nature Geoscience, v. 10, p. 51–57, https://doi.org/10.1038/ngeo2857.
Fagereng, Å., and Diener, J.F.A., 2011, Non-volcanic tremor and discontinuous slab dehydration: Geophysical Research Letters, v. 38, no. 15, L15302, https://doi.org/10.1029/2011GL048214.
Fagereng, Å., and Harris, C., 2014, Interplay between fluid flow and fault-fracture mesh generation within underthrust sediments: Geochemical evidence from the Chrystalls Beach Complex, New Zealand: Tectonophysics, v. 612–613, p. 147–157, https://doi.org/10.1016/j.tecto.2013.12.002.
Fagereng, Å., Hillary, G.W.B., and Diener, J.F.A., 2014, Brittle-viscous deformation, slow slip, and tremor: Geophysical Research Letters, v. 41, no. 12, p. 4159–4167, https://doi.org/10.1002/2014GL060433.
Fagereng, Å., Remitti, F., and Sibson, R.H., 2011, Incrementally developed slickenfibers—Geological record of repeating low stress-drop seismic events?: Tectonophysics, v. 510, no. 3–4, p. 381–386, https://doi.org/10.1016/j.tecto.2011.08.015.
Farge, G., Shapiro, N.M., and Frank, W.B., 2020, Moment-duration scaling of low-frequency earthquakes in Guerrero, Mexico: Journal of Geophysical Research: Solid Earth, v. 125, https://doi.org/10.1029/2019JB019099.
Fisher, D.M., and Brantley, S.L., 2014, The role of silica redistribution in the evolution of slip instabilities along subduction interfaces: Constraints from the Kodiak accretionary complex, Alaska: Journal of Structural Geology, v. 69, p. 395–414, https://doi.org/10.1016/j.jsg.2014.03.010.
Fisher, D.M., Brantley, S.L., Everett, M., and Dzvonik, J., 1995, Cyclic fluid flow through a regionally extensive fracture network within the Kodiak accretionary prism: Journal of Geophysical Research: Solid Earth, v. 100, no. 12, p. 12,881–12,894, https://doi.org/10.1029/94JB02816.
Frank, W.B., and Brodsky, E.E., 2019, Daily measurement of slow slip from low-frequency earthquakes is consistent with ordinary earthquake scaling: Science Advances, v. 5, https://doi.org/10.1126/sciadv.aaw9386.
Frank, W.B., Shapiro, N.M., Husker, A.L., Kostoglodov, V., Romanenko, A., and Campillo, M., 2014, Using systematically characterized low-frequency earthquakes as a fault probe in Guerrero, Mexico: Journal of Geophysical Research: Solid Earth, v. 119, p. 7686–7700, https://doi.org/10.1002/2014JB011457.
Frank, W.B., Shapiro, N.M., Husker, A.L., Kostoglodov, V., Bhat, H.S., and Campillo, M., 2015a, Along-fault pore-pressure evolution during a slow-slip event in Guerrero, Mexico: Earth and Planetary Science Letters, v. 413, p. 135–143, https://doi.org/10.1016/j.epsl.2014.12.051.
Frank, W.B., Radiguet, M., Rousset, B., Shapiro, N.M., Husker, A.L., Kostoglodov, V., Cotte, N., and Campillo, M., 2015b, Uncovering the geodetic signature of silent slip through repeating earthquakes: Geophysical Research Letters, v. 42, p. 2774–2779, https://doi.org/10.1002/2015GL063685.
Frank, W.B., Shapiro, N.M., Husker, A.L., Kostoglodov, V., Gusev, A.A., and Campillo, M., 2016, The evolving interaction of low-frequency earthquakes during transient slip: Science Advances, v. 2, https://doi.org/10.1126/sciadv.1501616.
Frank, W.B., Rousset, B., Lasserre, C., and Campillo, M., 2018, Revealing the cluster of slow transients behind a large slow slip event: Science Advances, v. 4, https://doi.org/10.1126/sciadv.aat0661.
French, M.E., and Condit, C.B., 2019, Slip partitioning along an idealized subduction plate boundary at deep slow slip conditions: Earth and Planetary Science Letters, v. 528, https://doi.org/10.1016/j.epsl.2019.115828.
French, M.E., and Zhu, W., 2017, Slow fault propagation in serpentinite under conditions of high pore fluid pressure: Earth and Planetary Science Letters, v. 473, p. 131–140, https://doi.org/10.1016/j.epsl.2017.06.009.
Fusseis, F., Handy, M.R., and Schrank, C., 2006, Networking of shear zones at the brittle-to-viscous transition (Cap de Creus, NE Spain): Journal of Structural Geology, v. 28, p. 1228–1243, https://doi.org/10.1016/j.jsg.2006.03.022.
Gao, H., Schmidt, D.A., and Weldon, R.J., 2012, Scaling relationships of source parameters for slow slip events: Bulletin of the Seismological Society of America, v. 102, no. 1, p. 352–360, https://doi.org/10.1785/0120110096.
Gao, X., and Wang, K., 2017, Rheological separation of the megathrust seismogenic zone and episodic tremor and slip: Nature, v. 543, no. 7645, p. 416–419, https://doi.org/10.1038/nature21389.
Gardner, R., Piazolo, S., Evans, L., and Daczko, N., 2017, Patterns of strain localization in heterogeneous, polycrystalline rocks—A numerical perspective: Earth and Planetary Science Letters, v. 463, p. 253–265, https://doi.org/10.1016/j.epsl.2017.01.039.
Geller, R., and Mueller, C., 1980, Four similar earthquakes in central California: Geophysical Research Letters, v. 7, p. 821–824, https://doi.org/10.1029/GL007i010p00821.
Giuntoli, F., and Viola, G., 2022, A likely geological record of deep tremor and slow slip events from a subducted continental broken formation: Scientific Reports, v. 12, no. 1, https://doi.org/10.1038/s41598-022-08489-2.
Gomberg, J., Wech, A., Creager, K., Obara, K., and Agnew, D., 2016, Reconsidering earthquake scaling: Geophysical Research Letters, v. 43, p. 6243–6251, https://doi.org/10.1002/2016GL069967.
Guillot, S., Schwartz, S., Reynard, B., Agard, P., and Prigent, C., 2015, Tectonic significance of serpentinites: Tectonophysics, v. 646, p. 1–19, https://doi.org/10.1016/j.tecto.2015.01.020.
Hawthorne, J.C., and Rubin, A.M., 2013, Laterally propagating slow slip events in a rate and state friction model with a velocity-weakening to velocity-strengthening transition: Journal of Geophysical Research: Solid Earth, v. 118, p. 3785–3808, https://doi.org/10.1002/jgrb.50261.
Hayman, N.W., and Lavier, L.L., 2014, The geologic record of deep episodic tremor and slip: Geology, v. 42, p. 195–198, https://doi.org/10.1130/G34990.1.
Hirose, H., Hirahara, K., Kimata, F., Fujii, N., and Miyazaki, S., 1999, A slow thrust slip event following the two 1996 Hyuganada earthquakes beneath the Bungo Channel, southwest Japan: Geophysical Research Letters, v. 26, p. 3237–3240, https://doi.org/10.1029/1999GL010999.
Hirth, G., and Guillot, S., 2013, Rheology and tectonic significance of serpentinite: Elements, v. 9, p. 107–113, https://doi.org/10.2113/gselements.9.2.107.
Hitz, B., and Wakabayashi, J., 2012, Unmetamorphosed sedimentary mélange with high-pressure metamorphic blocks in a nascent forearc basin setting: Tectonophysics, v. 568–569, p. 124–134, https://doi.org/10.1016/j.tecto.2011.12.006.
Hoover, W.F., Condit, C.B., Lindquist, P.C., Moser, A.C., and Guevara, V.E., 2022a, Episodic slow slip hosted by talc-bearing metasomatic rocks: High strain rates and stress amplification in a chemically reacting shear zone: Geophysical Research Letters, v. 49, https://doi.org/10.1029/2022GL101083.
Hoover, W.F., Penniston-Dorland, S., Baumgartner, L., Bouvier, A.-S., Dragovic, B., Locatelli, M., Angiboust, S., and Agard, P., 2022b, Episodic fluid flow in an eclogite-facies shear zone: Insights from Li isotope zoning in garnet: Geology, v. 50, p. 746–750, https://doi.org/10.1130/G49737.1.
Houston, H., 2015, Low friction and fault weakening revealed by rising sensitivity of tremor to tidal stress: Nature Geoscience, v. 8, p. 409–415, https://doi.org/10.1038/ngeo2419.
Houston, H., Delbridge, B.G., Wech, A.G., and Creager, K.C., 2011, Rapid tremor reversals in Cascadia generated by a weakened plate interface: Nature Geoscience, v. 4, p. 404–409, https://doi.org/10.1038/ngeo1157.
Ide, S., Beroza, G.C., Shelly, D.R., and Uchide, T., 2007a, A scaling law for slow earthquakes: Nature, v. 447, no. 7140, p. 76–79, https://doi.org/10.1038/nature05780.
Ide, S., Shelly, D.R., and Beroza, G.C., 2007b, Mechanism of deep low frequency earthquakes: Further evidence that deep non-volcanic tremor is generated by shear slip on the plate interface: Geophysical Research Letters, v. 34, p. 2191–2195, https://doi.org/10.1029/2006GL028890.
Ikari, M.J., Marone, C., Saffer, D.M., and Kopf, A.J., 2013, Slip weakening as a mechanism for slow earthquakes: Nature Geoscience, v. 6, no. 6, p. 468–472, https://doi.org/10.1038/ngeo1818.
Im, K., Saffer, D., Marone, C., and Avouac, J.P., 2020, Slip-rate-dependent friction as a universal mechanism for slow slip events: Nature Geoscience, v. 13, p. 705–710, https://doi.org/10.1038/s41561-020-0627-9.
Johnson, K.M., Shelly, D.R., and Bradley, A.M., 2013, Simulations of tremor-related creep reveal a weak crustal root of the San Andreas fault: Geophysical Research Letters, v. 40, p. 1300–1305, https://doi.org/10.1002/grl.50216.
Kaus, B.J.P., and Podladchikov, Y.Y., 2006, Initiation of localized shear in visco-elasto-plastic rocks: Journal of Geophysical Research: Solid Earth, v. 111, B04412, https://doi.org/10.1029/2005JB003652.
Kimura, G., Yamaguchi, A., Hojo, M., Kitamura, Y., Kameda, J., Ujiie, K., Hamada, Y., Hamahashi, M., and Hina, S., 2012, Tectonic mélange as fault rock of subduction plate boundary: Tectonophysics, v. 568–569, p. 25–38, https://doi.org/10.1016/j.tecto.2011.08.025.
Kirkpatrick, J.D., Fagereng, Å., and Shelly, D.R., 2021, Geological constraints on the mechanisms of slow earthquakes: Nature Reviews Earth & Environment, v. 2, p. 285–301, https://doi.org/10.1038/s43017-021-00148-w.
Kitajima, H., and Saffer, D.M., 2012, Elevated pore pressure and anomalously low stress in regions of low frequency earthquakes along the Nankai Trough subduction megathrust: Geophysical Research Letters, v. 39, L23301, https://doi.org/10.1029/2012GL053793.

Kitamura, Y., Sato, K., Ikesawa, E., Ikehara-Ohmori, K., Kimura, G., Kondo, H., et al., 2005, Mélange and its seismogenic roof décollement: A plate boundary fault rock in the subduction zone—An example from the Shimanto Belt, Japan: Tectonics, v. 24, TC5012. https://doi.org/10.1029/2004TC001635.

Kotowski, A.J., and Behr, W.M., 2019, Length scales and types of heterogeneities along the deep subduction interface: Insights from exhumed rocks on Syros Island, Greece: Geosphere, v. 15, p. 1038–1065, https://doi.org/10.1130/GES02037.1.

Lanphere, M.A., Blake, M.C., and Irwin, W.P., 1978, Early Cretaceous metamorphic age of the South Fork Mountain Schist in the northern Coast Ranges of California: American Journal of Science, v. 278, p. 798–815, https://doi.org/10.2475/ajs.278.6.798.

Lavier, L.L., Tong, X., and Biemiller, J., 2021, The mechanics of creep, slow slip events, and earthquakes in mixed brittle-ductile fault zones: Journal of Geophysical Research: Solid Earth, v. 126, no. 2, https://doi.org/10.1029/2020JB020325.

Liu, Y., and Rice, J.R., 2007, Spontaneous and triggered aseismic deformation transients in a subduction fault model: Journal of Geophysical Research: Solid Earth, v. 112, no. B9, B09404, https://doi.org/10.1029/2007JB004930.

Lusk, A.D.J., and Platt, J.P., 2020, The deep structure and rheology of a plate boundary–scale shear zone: Constraints from an exhumed Caledonian shear zone, NW Scotland: Lithosphere, v. 2020, https://doi.org/10.2113/2020/8824736.

Mancktelow, N.S., and Pennacchioni, G., 2005, The control of precursor brittle fracture and fluid-rock interaction on the development of single and paired ductile shear zones: Journal of Structural Geology, v. 27, p. 645–661, https://doi.org/10.1016/j.jsg.2004.12.001.

Meneghini, F., and Moore, J.C., 2007, Deformation and hydrofracture in a subduction thrust at seismogenic depths: The Rodeo Cove thrust zone, Marin Headlands, California: Geological Society of America Bulletin, v. 119, p. 174–183, https://doi.org/10.1130/B25807.1.

Meneghini, F., Marroni, M., and Pandolfi, L., 2007, Fluid flow during accretion in sediment-dominated margins: Evidence of a high-permeability fossil fault zone from the Internal Ligurian accretionary units of the Northern Apennines, Italy: Journal of Structural Geology, v. 29, no. 3, p. 515–529, https://doi.org/10.1016/j.jsg.2006.10.003.

Miller, M.M., Melbourne, T., Johnson, D.J., and Sumner, W.Q., 2002, Periodic slow earthquakes from the Cascadia subduction zone: Science, v. 295, p. 2423, https://doi.org/10.1126/science.1071193.

Miyazawa, M., and Brodsky, E.E., 2008, Deep low-frequency tremor that correlates with passing surface waves: Journal of Geophysical Research: Solid Earth, v. 113, https://doi.org/10.1029/2006JB004890.

Moore, D.E., and Rymer, M.J., 2007, Talc bearing serpentinite and the creeping section of the San Andreas fault: Nature, v. 448, p. 795–797, https://doi.org/10.1038/nature06064.

Muñoz-Montecinos, J., and Behr, W.M., 2023, Transient permeability of a deep-seated subduction interface shear zone: Geophysical Research Letters, v. 50, https://doi.org/10.1029/2023GL104244.

Muto, J., Hirth, G., Heilbronner, R., and Tullis, J., 2011, Plastic anisotropy and fabric evolution in sheared and recrystallized quartz single crystals: Journal of Geophysical Research: Solid Earth, v. 116, B02206, https://doi.org/10.1029/2010JB007891.

Nishikawa, T., Ide, S., and Nishimura, T., 2023, A review on slow earthquakes in the Japan Trench: Progress in Earth and Planetary Science, v. 10, p. 1–51, https://doi.org/10.1186/s40645-022-00528-w.

Nishiyama, N., Sumino, H., and Ujiie, K., 2020, Fluid overpressure in subduction plate boundary caused by mantle-derived fluids: Earth and Planetary Science Letters, v. 538, https://doi.org/10.1016/j.epsl.2020.116199.

Obara, K., 2002, Nonvolcanic deep tremor associated with subduction in southwest Japan: Science, v. 296, no. 5573, p. 1679–1681, https://doi.org/10.1126/science.1070378.

Peacock, S.M., Christensen, N.I., Bostock, M.G., and Audet, P., 2011, High pore pressures and porosity at 35 km depth in the Cascadia subduction zone: Geology, v. 39, p. 471–474, https://doi.org/10.1130/G31649.1.

Peng, Z., and Gomberg, J., 2010, An integrated perspective of the continuum between earthquakes and slow-slip phenomena: Nature Geoscience, v. 3, no. 9, p. 599–607, https://doi.org/10.1038/ngeo940.

Penniston-Dorland, S.C., Bebout, G.E., von Strandmann, P.A.P., Elliott, T., and Sorensen, S.S., 2012, Lithium and its isotopes as tracers of subduction zone fluids and metasomatic processes: Evidence from the Catalina Schist, California, USA: Geochimica et Cosmochimica Acta, v. 77, p. 530–545, https://doi.org/10.1016/j.gca.2011.10.038.

Phillips, N.J., Motohashi, G., Ujiie, K., and Rowe, C.D., 2020a, Evidence of localized failure along altered basaltic blocks in tectonic mélange at the updip limit of the seismogenic zone: Implications for the shallow slow earthquake source: Geochemistry, Geophysics, Geosystems, v. 21, no. 7, https://doi.org/10.1029/2019GC008839.

Phillips, N.J., Belzer, B., French, M.E., Rowe, C.D., and Ujiie, K., 2020b, Frictional strength of subduction thrust rocks in the region of shallow slow earthquakes: Journal of Geophysical Research: Solid Earth, v. 125, https://doi.org/10.1029/2019JB018888.

Platt, J.P., 2000, Calibrating the bulk rheology of active obliquely convergent thrust and accretionary wedges from surface profiles and velocity distributions: Tectonics, v. 19, p. 529–548, https://doi.org/10.1029/1999TC001121.

Platt, J.P., 2015, Origin of Franciscan blueschist-bearing mélange at San Simeon, central California coast: International Geology Review, v. 57, p. 843–853, https://doi.org/10.1080/00206814.2014.902756.

Platt, J.P., and Behr, W.M., 2011, Grainsize evolution in ductile shear zones: Implications for strain localization and the strength of the lithosphere: Journal of Structural Geology, v. 33, p. 537–550, https://doi.org/10.1016/j.jsg.2011.01.018.

Platt, J.P., and Schmidt, W.L., 2024, Is the inverted field gradient in the Catalina Schist terrane primary or constructional?: Tectonics, v. 43, no. 2, https://doi.org/10.1029/2023TC008021.

Platt, J.P., Leggett, J.K., and Alam, S., 1988, Slip vectors and fault mechanics in the Makran accretionary wedge, SW Pakistan: Journal of Geophysical Research: Solid Earth, v. 93, p. 7955–7973, https://doi.org/10.1029/JB093iB07p07955.

Platt, J.P., Xia, H., and Schmidt, W.L., 2018, Rheology and stress in subduction zones around the aseismic/seismic transition: Progress in Earth and Planetary Science, v. 5, no. 24, https://doi.org/10.1186/s40645-018-0183-8.

Platt, J.P., Grove, M., Kimbrough, D.L., and Jacobson, C.E., 2020, Structure, metamorphism, and geodynamic significance of the Catalina Schist terrane, *in* Heermance, R.V., and Schwartz, J.J., eds., From the Islands to the Mountains: A 2020 View of Geologic Excursions in Southern California: Geological Society of America Field Guide 59, p. 165–195, https://doi.org/10.1130/2020.0059(05).

Putnis, A., 2009, Mineral replacement reactions: Reviews in Mineralogy and Geochemistry, v. 70, no. 1, p. 87–124, https://doi.org/10.2138/rmg.2009.70.3.

Raimbourg, H., Famin, V., Palazzin, G., Yamaguchi, A., Augier, R., Kitamura, Y., and Sakaguchi, A., 2019, Distributed deformation along the subduction plate interface: The role of tectonic mélanges: Lithos, v. 334–335, p. 69–87, https://doi.org/10.1016/j.lithos.2019.01.033.

Ramsay, J.G., 1980, The crack-seal mechanism of rock deformation: Nature, v. 284, p. 135–139, https://doi.org/10.1038/284135a0.

Roberts, N.M., and Holdsworth, R.E., 2022, Timescales of faulting through calcite geochronology: A review: Journal of Structural Geology, v. 158, https://doi.org/10.1016/j.jsg.2022.104578 [Photo courtesy of Dr. Arito Sakaguchi].

Rogers, G., and Dragert, H., 2003, Episodic tremor and slip on the Cascadia subduction zone: The chatter of silent slip: Science, v. 300, no. 5627, p. 1942–1943, https://doi.org/10.1126/science.1084783.

Rousset, B., Bürgmann, R., and Campillo, M., 2019, Slow slip events in the roots of the San Andreas fault: Science Advances, v. 5, https://doi.org/10.1126/sciadv.aav3274.

Rowe, C.D., Moore, J.C., Meneghini, F., and McKiernan, A.W., 2005, Large-scale pseudotachylites and fluidized cataclasites from an ancient subduction thrust fault: Geology, v. 33, p. 937–940, https://doi.org/10.1130/G21856.1.

Rowe, C.D., Moore, J.C., Remitti, F., and Scientists, I.E.T., 2013, The thickness of subduction plate boundary faults from the seafloor into the seismogenic zone: Geology, v. 41, p. 991–994, https://doi.org/10.1130/G34556.1.

Rubin, A.M., 2008, Episodic slow slip events and rate-and-state friction: Journal of Geophysical Research: Solid Earth, v. 113, B11414, https://doi.org/10.1029/2008JB005642.

Rubin, A.M., and Ampuero, J.P., 2005, Earthquake nucleation on (aging) rate and state faults: Journal of Geophysical Research: Solid Earth, v. 110, B11312, https://doi.org/10.1029/2005JB003686.

Saffer, D., and Tobin, H.J., 2011, Hydrogeology and mechanics of subduction zone forearcs: Fluid flow and pore pressure: Annual Review of Earth and Planetary Sciences, v. 39, p. 157–186, https://doi.org/10.1146/annurev-earth-040610-133408.

Saffer, D.M., and Wallace, L.M., 2015, The frictional, hydrologic, metamorphic and thermal habitat of shallow slow earthquakes: Nature Geoscience, v. 8, p. 594–600, https://doi.org/10.1038/ngeo2490.

Savard, G., Bostock, M.G., and Christensen, N.I., 2018, Seismicity, metamorphism, and fluid evolution across the northern Cascadia fore arc: Geochemistry, Geophysics, Geosystems, v. 19, p. 1881–1897, https://doi.org/10.1029/2017GC007417.

Schmidt, W.L., and Platt, J.P., 2018, Subduction, accretion, and exhumation of coherent Franciscan blueschist-facies rocks, northern Coast Ranges, California: Lithosphere, v. 10, p. 301–326, https://doi.org/10.1130/L697.1.

Schmidt, W.L., and Platt, J.P., 2020, Metamorphic temperatures and pressures across the eastern Franciscan: Implications for underplating and exhumation: Lithosphere, v. 2020, https://doi.org/10.2113/2020/8853351.

Schmidt, W.L., and Platt, J.P., 2022, Stress, microstructure, and deformation mechanisms during subduction underplating at the depth of tremor and slow slip, Franciscan Complex, northern California: Journal of Structural Geology, v. 154, https://doi.org/10.1016/j.jsg.2021.104469.

Scholl, D.W., 2019, Seismic imaging evidence that forearc underplating built the accretionary rock record of coastal North and South America: Geological Magazine, v. 158, p. 104–117, https://doi.org/10.1017/S0016756819000955.

Segall, P., Rubin, A.M., Bradley, A.M., and Rice, J.R., 2010, Dilatant strengthening as a mechanism for slow slip events: Journal of Geophysical Research: Solid Earth, v. 115, B12305, https://doi.org/10.1029/2010JB007449.

Shelly, D.R., 2009, Possible deep fault slip preceding the 2004 Parkfield earthquake, inferred from detailed observations of tectonic tremor: Geophysical Research Letters, v. 36, L17318, https://doi.org/10.1029/2009GL039589.

Shelly, D.R., Beroza, G.C., and Ide, S., 2007, Non-volcanic tremor and low-frequency earthquake swarms: Nature, v. 446, p. 305–307, https://doi.org/10.1038/nature05666.

Sibson, R.H., 2017, Tensile overpressure compartments on low-angle thrust faults: Earth, Planets, and Space, v. 69, https://doi.org/10.1186/s40623-017-0699-y.

Smith, D.L., and Evans, B., 1984, Diffusional crack healing in quartz: Journal of Geophysical Research: Solid Earth, v. 89, no. B6, p. 4125–4135, https://doi.org/10.1029/JB089iB06p04125.

Smith, R.B., 1977, Formation of folds, boudinage, and mullions in non-Newtonian materials: Geological Society of America Bulletin, v. 88, p. 312–320, https://doi.org/10.1130/0016-7606(1977)88<312:FOFBAM>2.0.CO;2.

Spandler, G., and Hermann, J., 2006, High-pressure veins in eclogite from New Caledonia and their significance for fluid migration in subduction zones: Lithos, v. 89, p. 135–153, https://doi.org/10.1016/j.lithos.2005.12.003.

Svahnberg, H., and Piazolo, S., 2010, The initiation of strain localisation in plagioclase-rich rocks: Insights from detailed microstructural analyses: Journal of Structural Geology, v. 32, p. 1404–1416, https://doi.org/10.1016/j.jsg.2010.06.011.

Sweet, J.R., Creager, K.C., and Houston, H., 2014, A family of repeating low-frequency earthquakes at the downdip edge of tremor and slip: Geochemistry, Geophysics, Geosystems, v. 15, no. 9, p. 3713–3721, https://doi.org/10.1002/2014GC005449.

Taetz, S., John, T., Bröcker, M., and Spandler, C., 2016, Fluid-rock interaction and evolution of a high-pressure/low-temperature vein system in eclogite from New Caledonia: Insights into intraslab fluid flow processes: Contributions to Mineralogy and Petrology, v. 171, https://doi.org/10.1007/s00410-016-1295-z.

Taetz, S., John, T., Bröcker, M., Spandler, C., and Stracke, A., 2018, Fast intraslab fluid-flow events linked to pulses of high pore fluid pressure at the subducted plate interface: Earth and Planetary Science Letters, v. 482, p. 33–43, https://doi.org/10.1016/j.epsl.2017.10.044.

Tamaribuchi, K., Ogiso, M., and Noda, A., 2022, Spatiotemporal distribution of shallow tremors along the Nankai Trough, southwest Japan, as determined from waveform amplitudes and cross-correlations: Journal of Geophysical Research: Solid Earth, v. 127, https://doi.org/10.1029/2022JB024403.

Tarling, M.S., Smith, S.A.F., Scott, J.M., Rooney, J.S., Viti, C., and Gordon, K.C., 2019, The internal structure and composition of a plate-boundary-scale serpentinite shear zone: The Livingstone fault, New Zealand: Solid Earth, v. 10, no. 4, p. 1025–1047, https://doi.org/10.5194/se-10-1025-2019.

Tewksbury-Christle, C.M., Behr, W.M., and Helper, M.A., 2021, Tracking deep sediment underplating in a fossil subduction margin: Implications for interface rheology and mass and volatile recycling: Geochemistry, Geophysics, Geosystems, v. 22, https://doi.org/10.1029/2020GC009463.

Thomas, A.M., Nadeau, R.M., and Bürgmann, R., 2009, Tremor-tide correlations and near-lithostatic pore pressure on the deep San Andreas fault: Nature, v. 462, no. 7276, p. 1048–1051, https://doi.org/10.1038/nature08654.

Thomas, A.M., Beroza, G.C., and Shelly, D.R., 2016, Constraints on the source parameters of low-frequency earthquakes on the San Andreas fault: Geophysical Research Letters, v. 43, p. 1464–1471, https://doi.org/10.1002/2015GL067173.

Tulley, C.J., Fagereng, Å., Ujiie, K., Piazolo, S., Tarling, M.S., and Mori, Y., 2022, Rheology of naturally deformed antigorite serpentinite: Strain and strain-rate dependence at mantle-wedge conditions: Geophysical Research Letters, v. 49, https://doi.org/10.1029/2022GL098945.

Uchida, N., and Bürgmann, R., 2019, Repeating earthquakes: Annual Review of Earth and Planetary Sciences, v. 47, p. 305–332, https://doi.org/10.1146/annurev-earth-053018-060119.

Uenishi, K., and Rice, J.R., 2003, Universal nucleation length for slip-weakening rupture instability under nonuniform fault loading: Journal of Geophysical Research: Solid Earth, v. 108, 2042, https://doi.org/10.1029/2001JB001681.

Ujiie, K., Saishu, H., Fagereng, Å., Nishiyama, N., Otsubo, M., Masuyama, H., and Kagi, H., 2018, An explanation of episodic tremor and slow slip constrained by crack-seal veins and viscous shear in subduction mélange: Geophysical Research Letters, v. 45, p. 5371–5379, https://doi.org/10.1029/2018GL078374.

Ukar, E., and Cloos, M., 2014, Low-temperature blueschist-facies mafic blocks in the Franciscan mélange, San Simeon, California: Field relations, petrology, and counterclockwise *P-T* paths: Geological Society of America Bulletin, v. 126, p. 831–856, https://doi.org/10.1130/B30876.1.

Van Noten, K., and Sintubin, M., 2010, Linear to non-linear relationship between vein spacing and layer thickness in centimetre- to decimetre-scale siliciclastic multilayers from the High-Ardenne slate belt (Belgium, Germany): Journal of Structural Geology, v. 32, p. 377–391, https://doi.org/10.1016/j.jsg.2010.01.011.

Verberne, B.A., Chen, J., Niemeijer, A.R., de Bresser, J.H.P., Pennock, G.M., Drury, M.R., and Spiers, C.J., 2017, Microscale cavitation as a mechanism for nucleating earthquakes at the base of the seismogenic zone: Nature Communications, v. 8, 1645, https://doi.org/10.1038/s41467-017-01843-3.

Vidale, J., Ellsworth, W., Cole, A., and Marone, C., 1994, Variations in rupture process with recurrence interval in a repeated small earthquake: Nature, v. 368, p. 624–626, https://doi.org/10.1038/368624a0.

Wakabayashi, J., and Dilek, Y., 2011, Mélanges of the Franciscan Complex, California: Diverse structural settings, evidence for sedimentary mixing, and their connection to subduction processes, *in* Wakabayashi, J., and Dilek, Y., eds., Mélanges: Processes of Formation and Societal Significance: Geological Society of America Special Paper 480, p. 117–141, https://doi.org/10.1130/2011.2480(05).

Wallace, L.M., 2020, Slow slip events in New Zealand: Annual Review of Earth and Planetary Sciences, v. 48, p. 175–203, https://doi.org/10.1146/annurev-earth-071719-055104.

Wallis, S.R., Yamaoka, K., Mori, H., Ishiwatari, A., Miyazaki, K., and Ueda, H., 2020, The basement geology of Japan from A to Z: The Island Arc, v. 29, https://doi.org/10.1111/iar.12339.

Wech, A.G., Boese, C.M., Stern, T.A., and Townend, J., 2012, Tectonic tremor and deep slow slip on the Alpine fault: Geophysical Research Letters, v. 39, L10303, https://doi.org/10.1029/2012GL051751.

Williams, R.T., and Fagereng, Å., 2022, The role of quartz cementation in the seismic cycle: A critical review: Reviews of Geophysics, v. 60, https://doi.org/10.1029/2021RG000768.

Wintsch, R.P., Christoffersen, R., and Kronenberg, A.K., 1995, Fluid-rock reaction weakening of fault zones: Journal of Geophysical Research: Solid Earth, v. 100, p. 13,021–13,032, https://doi.org/10.1029/94JB02622.

Xia, H., and Platt, J.P., 2017, Structural and rheological evolution of the Laramide subduction channel in southern California: Solid Earth, v. 8, p. 379–403, https://doi.org/10.5194/se-8-379-2017.

Xing, T., Zhu, W., French, M., and Belzer, B., 2019, Stabilizing effect of high pore fluid pressure on slip behaviors of gouge-bearing faults: Journal of Geophysical Research: Solid Earth, v. 124, p. 9526–9545, https://doi.org/10.1029/2019JB018002.